PREDICTED AND TESTED PERFORMANCE OF DURABLE TPS

John L. Shideler
NASA Langley Research Center
Hampton, VA

INTRODUCTION

The development of thermal protection systems (TPS) for aerospace vehicles involves combining material selection, concept design, and verification tests to evaluate the effectiveness of the system. The present paper reviews verification tests of two metallic and one carbon-carbon thermal protection system. The test conditions are, in general, representative of Space Shuttle design flight conditions which may be more or less severe than conditions required for future space transportation systems. The results of this study are intended to help establish a preliminary data base from which the designers of future entry vehicles can evaluate the applicability of future concepts to their vehicles.

SPACE SHUTTLE

The reusable surface insulation (RSI) selected for use on the Space Shuttle (fig. 1) was only one of many thermal protection concepts that were considered during the early shuttle design stages. One type of thermal protection that was considered was a radiative metallic system (ref. 1).

Figure 1

TYPICAL METALLIC THERMAL PROTECTION SYSTEM

The radiative stand-off thermal protection system shown in figure 2 (ref. 1) is typical of many of the metallic TPS concepts that were developed during the Space Shuttle design process. They consisted of a beaded or corrugated heat shield attached to flexible supports which were, in turn, attached to the vehicle structure. The heat shield protected fibrous insulation, which was usually encapsulated in a flexible package intended to be water-proof. Overlapping expansion joints accommodated thermal growth in the flow direction, and the beads or corrugations accommodated thermal growth in the direction transverse to the flow. Assembly of the heat shields and the stand-off supports to the vehicle structure required many fasteners. Therefore, the metallic concepts were perceived to be associated with high part count and to be heavy compared to the RSI. Consequently, at the time of Space Shuttle TPS concept selection, at least two of the factors that led to the rejection of the metallic systems were fabrication complexity and weight.

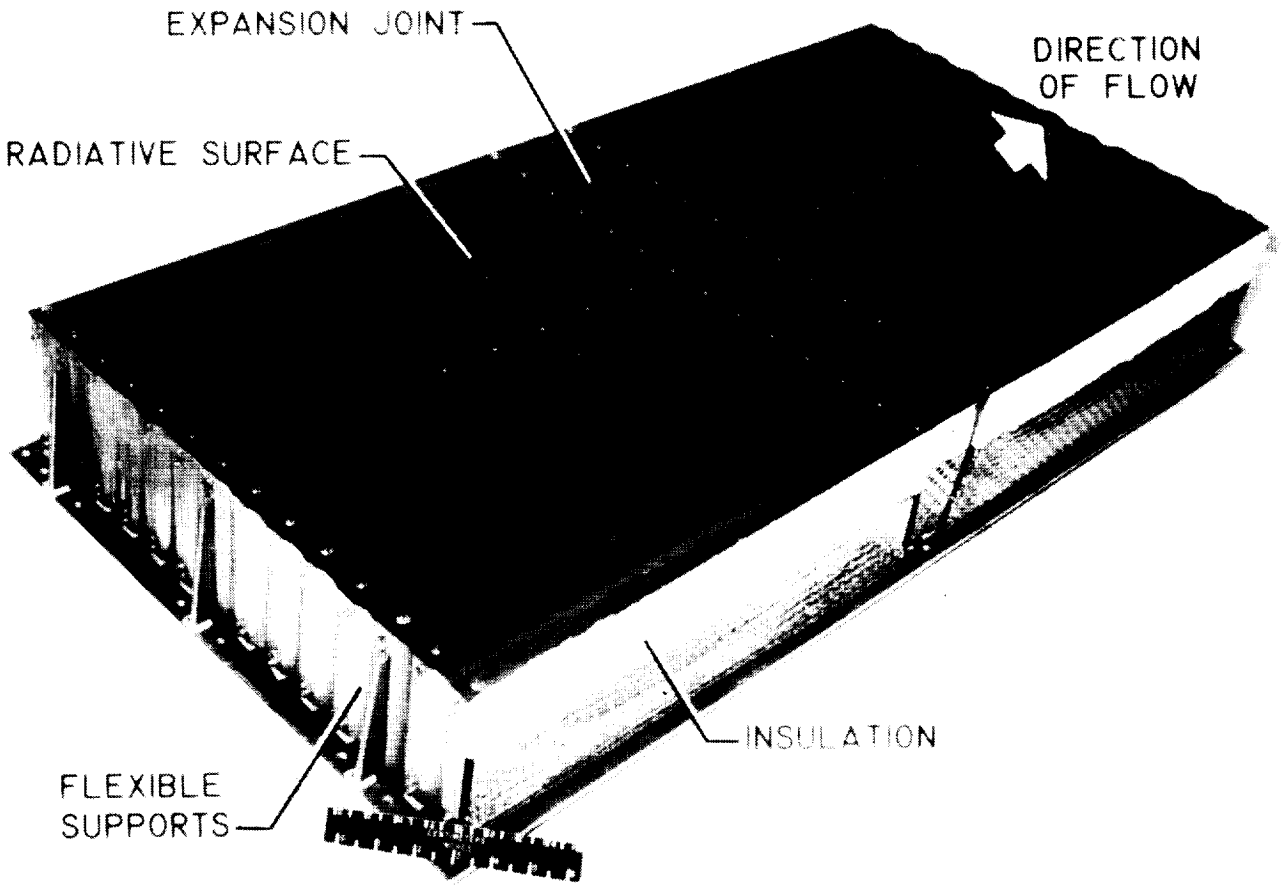

Figure 2

DURABLE TPS CONCEPTS

Although the RSI is an excellent insulator, it is very fragile. Titanium multiwall (M/W), superalloy honeycomb (SA/HC), and advanced carbon-carbon (ACC) multipost thermal protection system (TPS) concepts are being developed to provide more durable thermal protection for surfaces of future space transportation systems that operate at temperatures up to about 2300 ^{o} F. The two metallic prepackaged concepts shown in figure 3 are discrete panels that have a 1.0-in.-wide, 0.190-in.-thick strip of RTV-coated Nomex felt beneath the perimeter of each panel to prevent hot-gas flow beneath the panels. The ACC concept is a standoff design. The three concepts are described in detail in figures 4 and 5.

The goals of the TPS development program are to provide a durable surface of mechanically attached panels with overlapping edges that cover the gaps between the panels to reduce gap heating. As shown by the symbols in figure 3, these three concepts are mass competitive with the RSI TPS, the mass of which is indicated by the cross-hatched area.

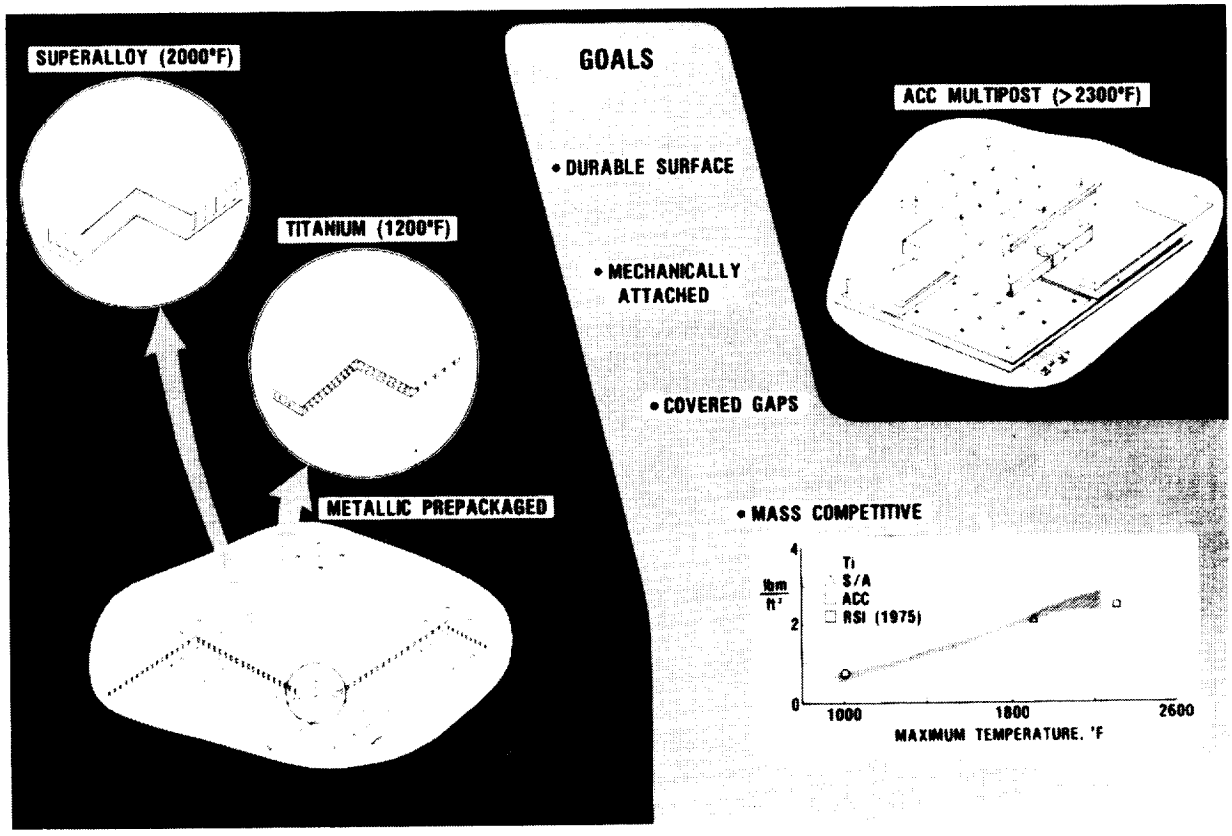

Figure 3

METALLIC TPS CONCEPTS

The titanium multiwall concept (See figure 4) consists of layers of dimpled 0.003-in.-thick titanium foil liquid-interface-diffusion (LID) bonded together at the dimples with a flat 0.0015-in.-thick foil sheet sandwiched between each dimpled sheet. The superalloy honeycomb concept consists of an Inconel 617 honeycomb outer surface panel with 0.005-in.-thick face sheets, layered fibrous insulation, and a titanium honeycomb inner surface panel with 0.006-in.-thick face sheets. The edges of the two metallic concepts are covered with 0.003-in.-thick beaded closures to form discrete panels nominally 12 in. square. The panels are vented by a 0.31-in.-diameter hole in the bottom that is covered with a 400-mesh screen. The titanium multiwall and superalloy honeycomb panels are described in detail in references 2 and 3, respectively.

The two types of attachments shown in figure 4 can be applied to either of the TPS concepts. The bayonet-clip attachment, shown with the titanium multiwall concept, consists of two clips and a metal tab (bayonet) LID bonded to the lower surface of the panel. One clip is mechanically attached to the vehicle surface and one clip is LID bonded to the lower surface of an adjacent panel. Thus, a single bayonet attaches a corner from each of two adjacent panels. The through-panel fastener, shown with the superalloy honeycomb concept, consists of a thin-walled Inconel 617 cylinder through the panel that allows access to a bolt which fastens the panel corner to the vehicle structure. The cylinder, which contains fibrous insulation, is covered with an Inconel 617 threaded plug. These fasteners are described in detail in reference 3.

The mass of the titanium multiwall panel designed for a location on the Space Shuttle with a maximum temperature of 1000° F is 0.806 lbm/ft^2 including bayonet attachments and uncoated Nomex felt, and the mass of the superalloy honeycomb panel designed for a location with a maximum surface temperature of 1900° F is 2.201 lbm/ft^2 including through-panel attachments and felt.

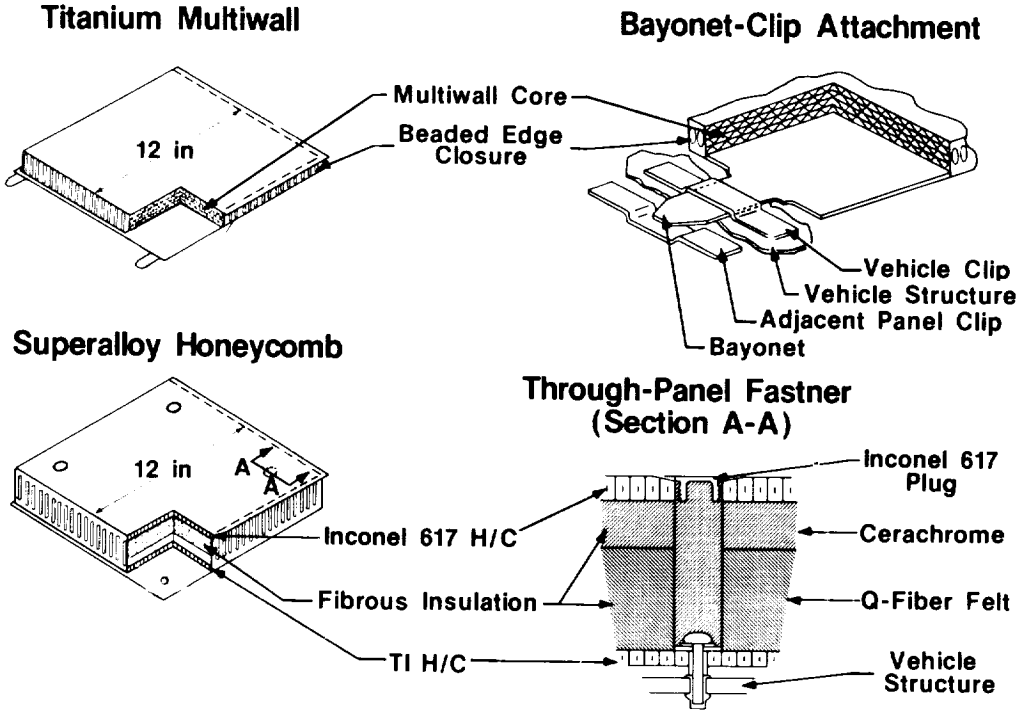

Figure 4

ADVANCED CARBON-CARBON MULTIPOST STANDOFF TPS CONCEPT

The advanced carbon-carbon multipost concept shown in figure 5 consists of a rib-stiffened ACC sheet attached to the vehicle primary structure by posts with fibrous insulation packaged in a ceramic cloth between the ACC panel and the vehicle structure. The surface of the single ACC panel is nominally 36 in. square. The ACC multipost concept is described in detail in reference 4, and fabrication of the ACC test model shown in later figures is described in reference 5.

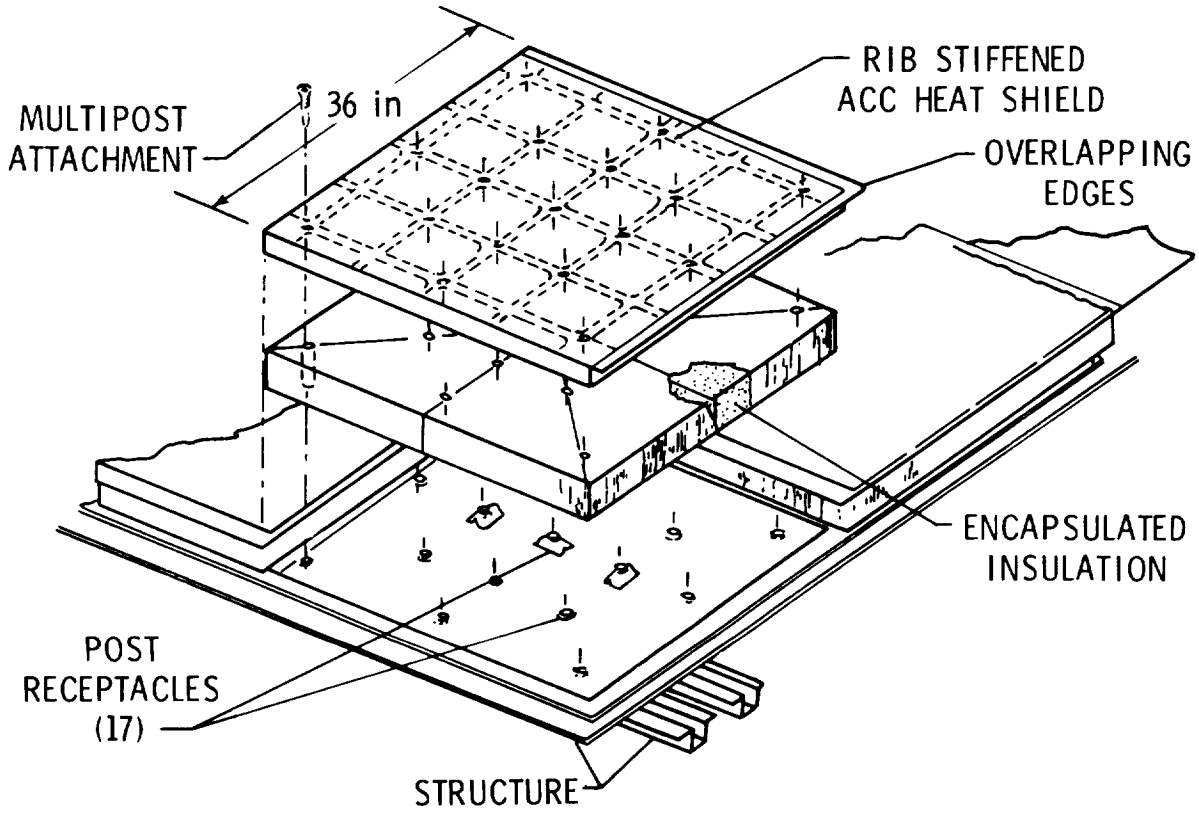

Figure 5

VERIFICATION TEST FACILITIES

NASA test facilities at Johnson Space Center (JSC), Kennedy Space Center (KSC), and Langley Research Center (LaRC) were used for verification tests of the three TPS concepts. The metallic concepts were exposed to thermal/vacuum, vibration, acoustic, environmental exposure, lightning strike, and wind tunnel tests. The ACC multipost concept was exposed to thermal/vacuum and arc tunnel tests. The test loads are, in general, representative of Space Shuttle design loads, which may be more or less severe than loads required for future space transportation systems.

TPS test models were exposed to combined temperature and pressure histories in thermal/vacuum test facilities at JSC, KSC, and LaRC to obtain thermal response characteristics of the concepts. In the facility at JSC, shown in figure 6, the heater system is mounted in a boiler-plate Apollo command module test chamber that is evacuated by a mechanical vacuum pump. The heater consists of electrically heated graphite elements enclosed in a fixture box purged with nitrogen.

Dynamic response of the metallic concepts was evaluated by shaker-table vibration tests, by acoustic exposure in a sound chamber at JSC, and by acoustic exposure in a progressive wave facility at LaRC. The acoustic exposure levels were representative of those experienced during Space Shuttle liftoff. The test panels were attached to the side wall of the test section of the LaRC facility shown in the figure. (The ACC test model was also exposed to thermal/vacuum tests in the facility. Graphite heaters are added to the test-section side wall opposite the test panel to provide radiant heating.)

Environmental tests to assess water retention and the effects of atmospheric contamination on metallic TPS were conducted near the KSC Space Shuttle launch site 39B shown in the figure. Lightning strike tests were conducted at LaRC to determine how much damage lightning impact caused on the metallic panels. The facility operates by charging a bank of capacitors and rapidly discharging the capacitors to a grounded test model. Arrays of metallic TPS panels were tested in the LaRC 8-foot High Temperature Tunnel (8'HTT), and an array of four corner segments of an ACC panel was tested in the LaRC 20 MW Aerothermal Arc Tunnel to evaluate the performance of the concepts in an aerothermal environment.

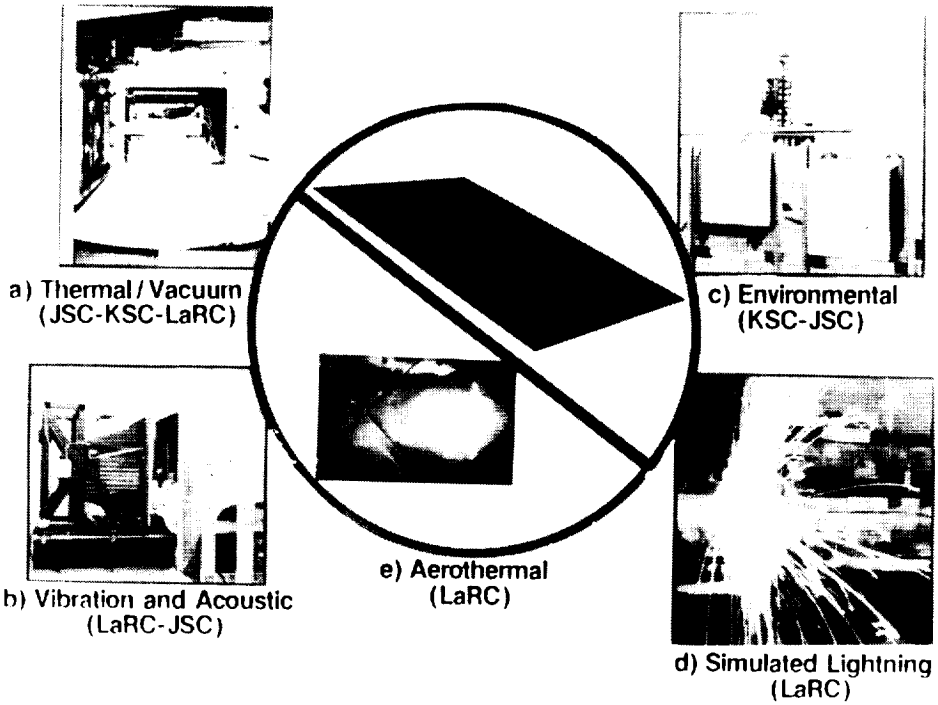

Figure 6

THERMAL/VACUUM TESTS

Typical results from the thermal vacuum tests of the titanium multiwall, superalloy honeycomb, and ACC panels are presented in figure 7. The panels were exposed to pressure histories in addition to temperature histories because the thermal conductivity of the fibrous insulation is a function of pressure. The surface temperature histories (lines 1) were imposed during the test and were used as input to a one-dimensional thermal analysis (ref. 6). Temperatures were calculated at thermocouple locations in the TPS (lines 2) and at aluminum plates (lines 3) that were sized to represent the thermal mass of a typical Space Shuttle structure where the TPS panels might be applied. The surface temperature histories for the titanium and superalloy panels are temperatures predicted at respective points on the Space Shuttle based on design trajectory 14414.1C. The measured back-surface temperatures on the metallic TPS models indicate acceptable thermal performance in that they did not exceed 350° F, the maximum allowable temperature for the aluminum structure. The ACC model was subjected to a surface temperature history similar to that expected for the arc tunnel tests. (The arc tunnel cannot provide the low heating rates that occur early in the shuttle entry trajectory.) The calculated temperatures were in reasonable agreement with the measured temperatures.

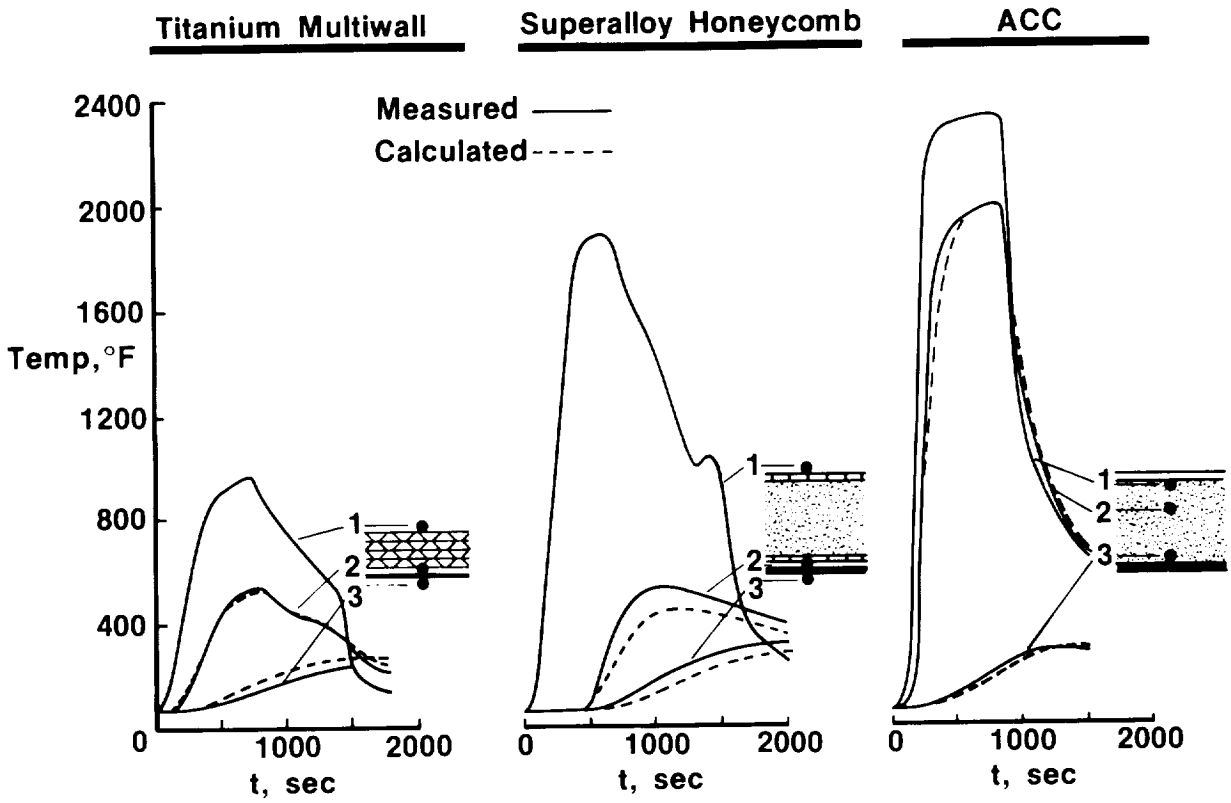

Figure 7

SUPERALLOY HONEYCOMB 2-PANEL ARRAY

The photograph to the left of figure 8 shows the superalloy honeycomb two-panel array before testing. The photograph on the right, taken at a different angle, shows the array after exposure to 25 thermal/vacuum cycles with a maximum surface temperature of 1900° F for each cycle. The array was exposed to one over-temperature test to 2000° F (cycle 26). No damage occurred to the panel; however, the central 4.5 in. of the overhanging lip covering the gap between panels buckled slightly. The amplitude of the buckle pattern was about 0.050 in. from crest to valley, and the wave length was about 1.5 in. from crest to crest. Such surface roughness is not expected to have an effect on the thermal performance of the TPS system because it would be within the boundary layer over most of the vehicle surface. The array was exposed to 161 dB for 15 minutes between cycles 16 and 17 (acoustic exposure is discussed later). No change in thermal performance occurred during these tests. Results from similar tests for the titanium multiwall two-panel array at temperatures up to 1200° F did not identify any deficiencies in the multiwall design.

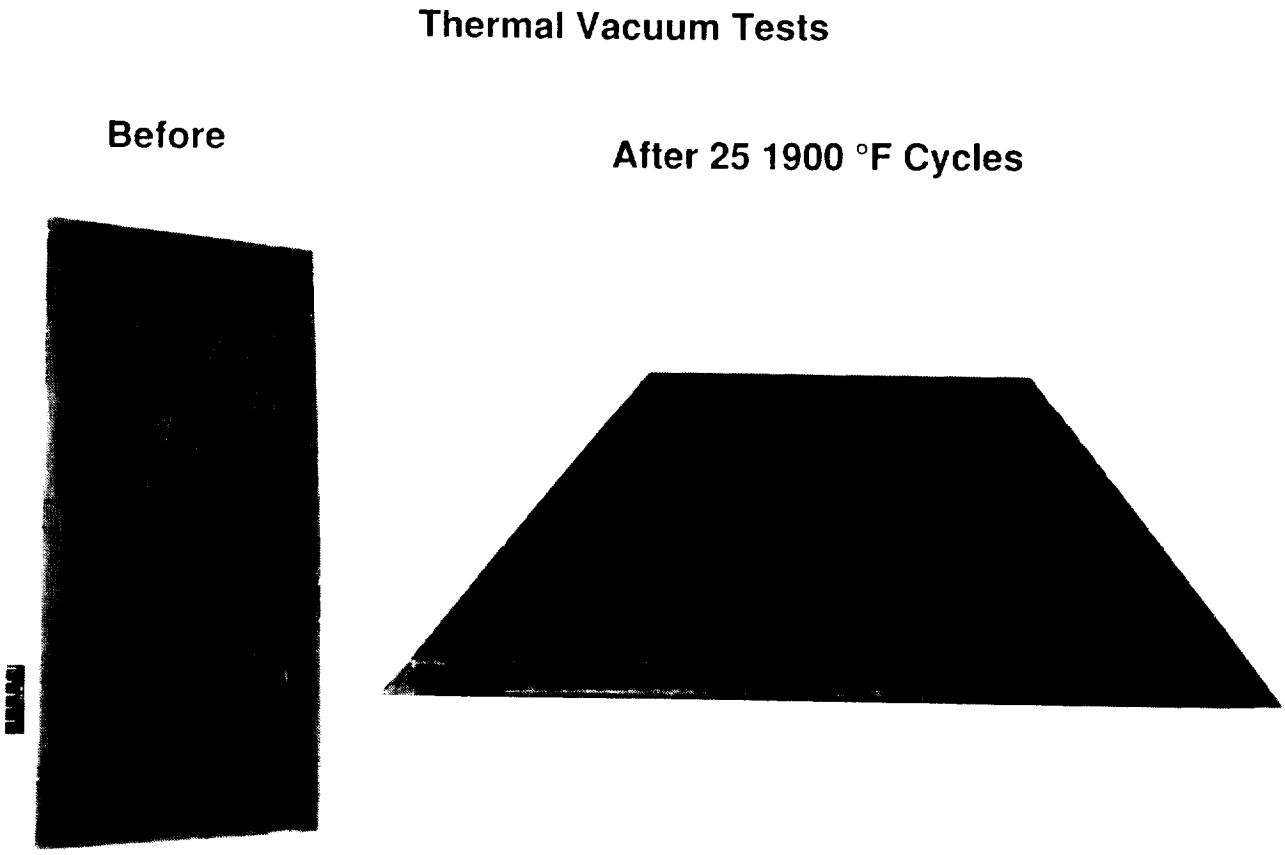

Figure 8

SHAKER-TABLE TESTS ON M/W AND SA/HC PANELS WITH THROUGH-PANEL FASTENERS

Titanium multiwall and superalloy honeycomb panels, each with through-panel attachments, were vibrated on an LaRC shaker table at three different g levels. The results of the tests are summarized in figure 9. The panels were exposed to 10 and 20 g levels of random vibration on each of three axes for 600 s/g-level. They were then exposed to 30 g's on each of three axes for 485 s. This exposure approximates 25 missions. The titanium multiwall panel was not damaged; however, the attachment screws on the superalloy panel became worn from repeated installation and removal. This wear caused the four fasteners to loosen during the last 30 g test and resulted in elongation of the fastener holes, the failure of two fasteners, and the bending of the other two. These results indicate that new screws should be used on reinstallation.

Concept	Exposure level (3-axes)	Time	Comments
Ti M/W	10 g's	600 sec/axes	Approximates 25 missions-- no damage
	20	600	
	30	485	
SA/HC	10 g's	600 sec/axes	Approximates 25 missions-- attachment screws worn from repeated disassembly
	20	600	
	30	485	

Figure 9

ACOUSTIC TESTS ON M/W AND SA/HC PANELS

Both the titanium multiwall and the superalloy honeycomb concepts were exposed to the acoustic environments shown in figure 10. Two facilities were used, a sound chamber at JSC operating at an overall sound pressure level (OASPL) of 161 dB and a progressive wave facility at LaRC operating at 159 dB. The spectrums are representative of the sound environment for the Space Shuttle at locations where the TPS concepts might be applied. Two-panel arrays tested at JSC had bayonet-clip attachments and were exposed to sound for 15 minutes, which is representative of about 25 missions with a scatter factor of 4. Single panels tested at LaRC had through-panel fasteners and were tested for 60 minutes, which corresponds to about 100 missions with a scatter factor of 4.

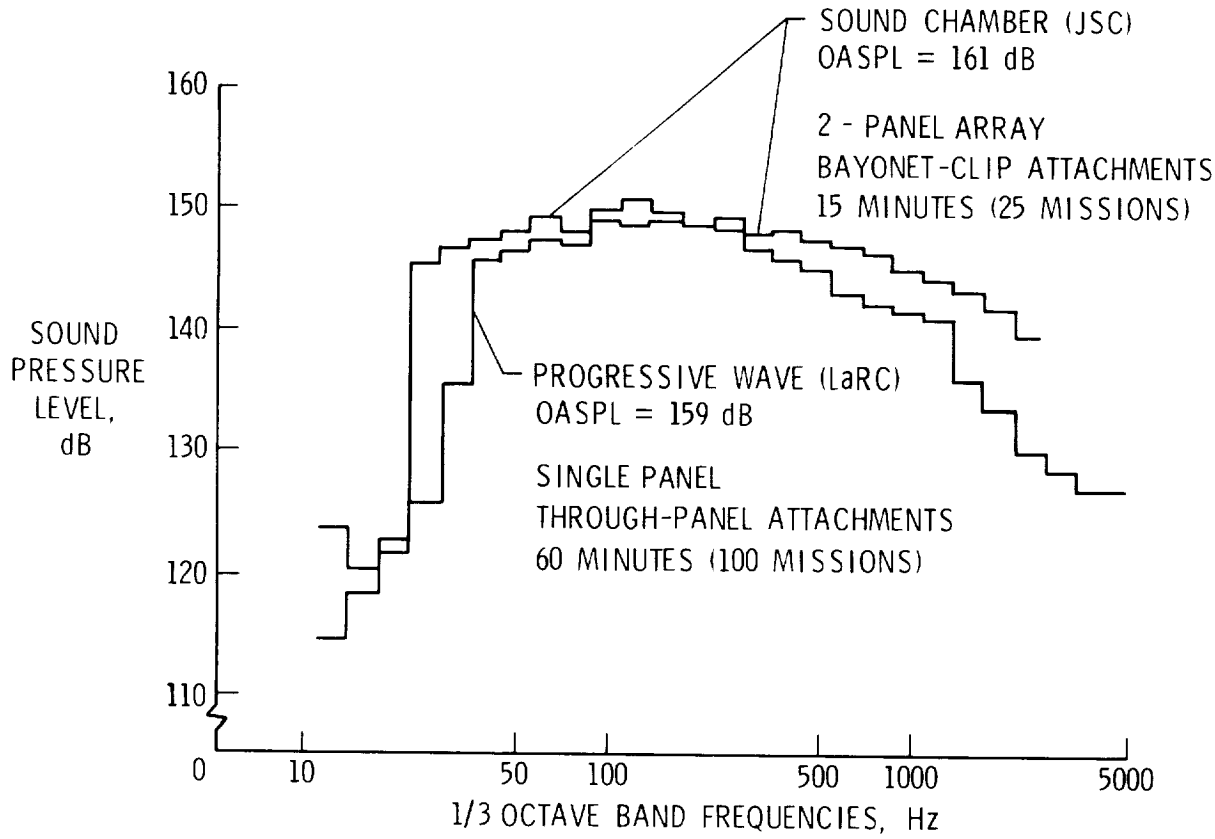

Figure 10

DAMAGE FROM ACOUSTIC TESTS OF SUPERALLOY HONEYCOMB PANELS

No damage occurred to the titanium multiwall panels in the tests in either of the facilities described in figure 10. However, the superalloy honeycomb panels sustained some damage in each facility. An edge view of one of the two superalloy honeycomb panels tested in the JSC sound chamber is shown in Figure 11. Prior to the test, the overhanging lip along the right half of the panel edge shown was bent down (in a pattern which fits a human hand), and some buckling along the bottom edge of the side closure occurred. Additionally, as identified in the figure, this edge was not properly supported by Nomex felt. All other edges were supported by a 1-in.-wide strip of Nomex felt as specified in the concept design. During the tests, numerous cracks occurred on the bottom edge of the unsupported side closure. Since the other seven side closures on the two panels suffered no damage during the tests, the cracks probably occurred due to the lack of felt support and handling damage.

One side closure of the superalloy honeycomb panel tested in the LaRC progressive wave facility was buckled in shipment. The panel was judged to be acceptable for vibration tests since the buckling was limited to only one edge. Upon completion of the vibration tests with no visible damage, the panel was exposed to acoustic load for 60 minutes. After the first 15 minutes, small cracks at the bottom of the buckled side closure were noticed. These cracks were monitored during the remaining acoustic exposure, but negligible growth occurred. A typical crack is shown in figure 11. Because the only damage was on the side buckled in shipment, the cracks that developed were probably due to the shipping damage.

Since the titanium multiwall panels showed no damage from the acoustic tests, and since the only cracks that developed on the superalloy honeycomb panels both at JSC and LaRC occurred in areas that had suffered handling damage prior to the tests, it appears that both concepts will survive sonic environments as high as 161 dB. However, demonstrated proof of survival would require additional acoustic tests.

a) Tested in JSC Sound Chamber

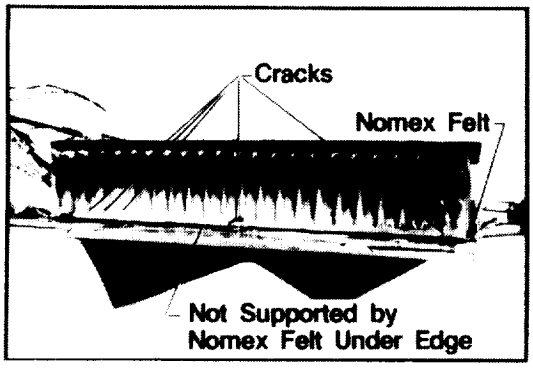

b) Tested LaRC Progressive Wave Facility

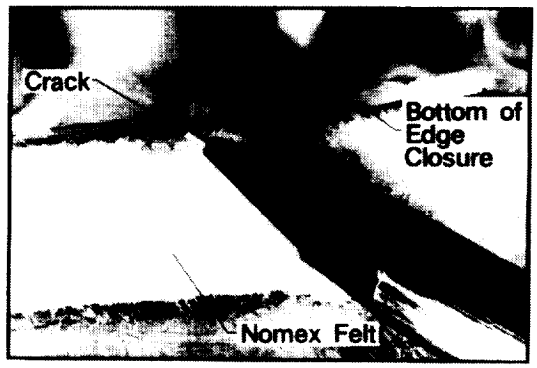

Figure 11

ENVIRONMENTAL EXPOSURE OF METALLIC PANELS AT KSC

Since thunderstorms occur frequently during the summer months at KSC and are characterized by heavy rainfall and occasional hail, environmental tests were designed to determine the water absorption/retention characteristics of multiwall TPS panels under actual rainfall conditions. Two first-generation titanium multiwall panels were exposed to the weather environment at Shuttle Launch Complex 39B at KSC shown in figure 12. Test results showed that water absorption is not a problem. During a three-month exposure period at the launch pad, no water was detected within the titanium multiwall panels. The water detection methods included measuring panel weight gain and using neutron radiography to detect small amounts of water.

Because KSC is near the Atlantic Ocean, salt and other contaminants can accumulate on the TPS surface over a period of time. Tests are planned to couple launch pad exposure with mission simulations to evaluate long-term environmental effects on metallic TPS. Current plans are to test titanium multiwall and superalloy honeycomb panels by subjecting them to repeated exposure to contaminants and thermal/vacuum cycles. During the test program, x-ray and other non-destructive techniques will be used to detect any physical changes with the metallic TPS.

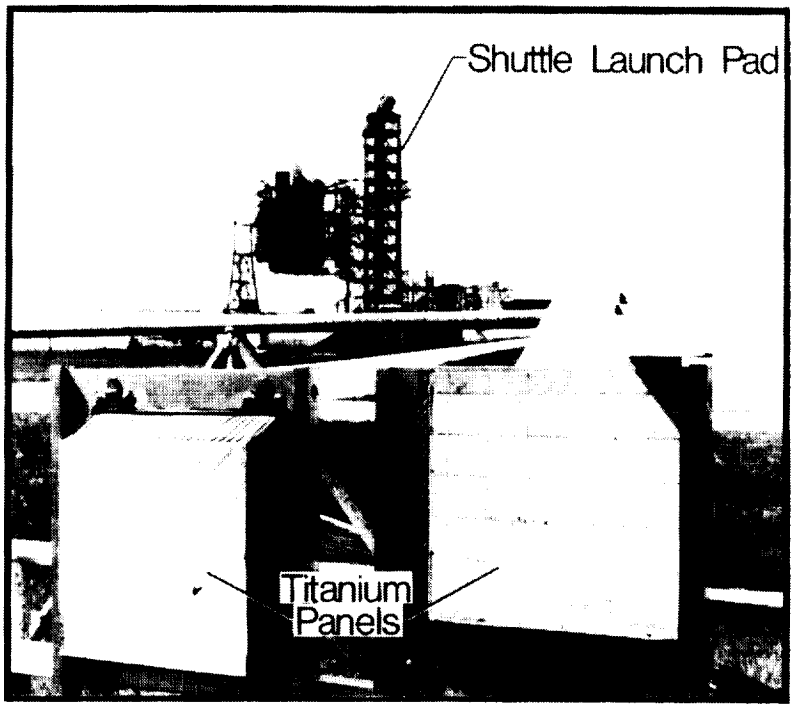

- **2-Week Exposure Cycles to Accumulate Contaminates**
- **Radiant Thermal/Vacuum Cycles to Simulate Mission Environment**
- **Repeat Exposure and Mission Cycles to Evaluate Long-Term Multi-Mission Effects**

Figure 12

SIMULATED LIGHTNING STRIKES ON METALLIC TPS

A titanium multiwall panel and a superalloy honeycomb panel were exposed to simulated lightning strikes. Damage from these tests is shown in figure 13. The strike on the titanium multiwall resulted in a conical hole through all the layers of the panel with a hole of approximately 1/8 inch in diameter in the lower surface. However, the damage to the superalloy honeycomb panel was limited to the Inconel surface. A spot on the surface of the panel about the size of a dime was indented as though it were hit with a ballpeen hammer. In addition, the face sheet was burned away locally, exposing two of the honeycomb cells. The intensity of these strikes (100 kA) meets the Space Shuttle criteria for lightning strikes on acreage surfaces (ref. 7).

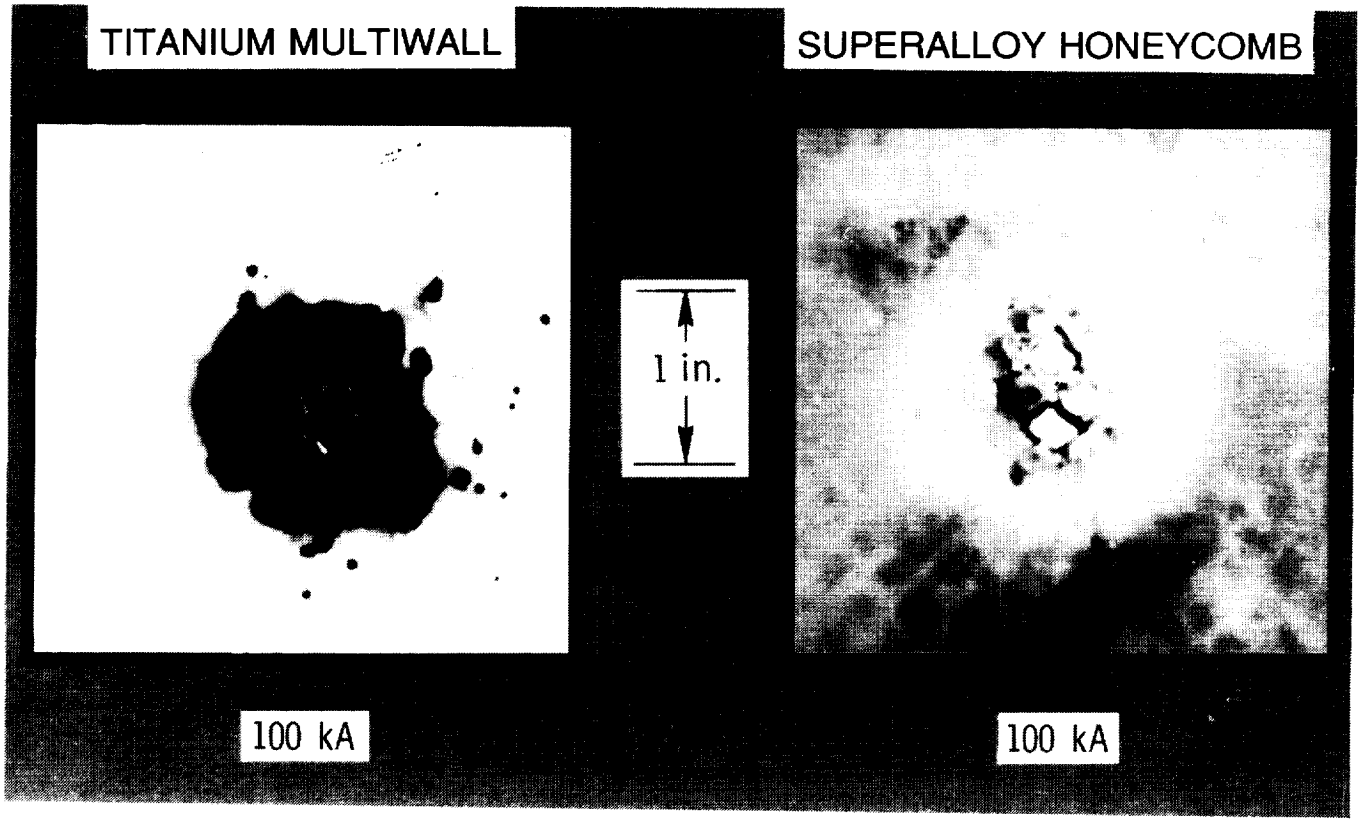

Figure 13

METALLIC TPS ARRAYS FOR 8-FT HTT TESTS

A titanium multiwall array of panels and a superalloy honeycomb array of panels were fabricated for radiant and aerothermal tests in the 8' High Temperature Tunnel (HTT) at LaRC. These arrays, shown in figure 14, consisted of 20 panels and were configured to fit a standard panel holder used in the 8' HTT. The panel holder has an opening, 60 in. by 42.5 in., and can accept test-specimen thicknesses up to about 12 inches. Since the standard metallic TPS panel is 12 in. square and the panel holder is 42.5 in. wide, panels approximately 6 in. wide were used to complete the array.

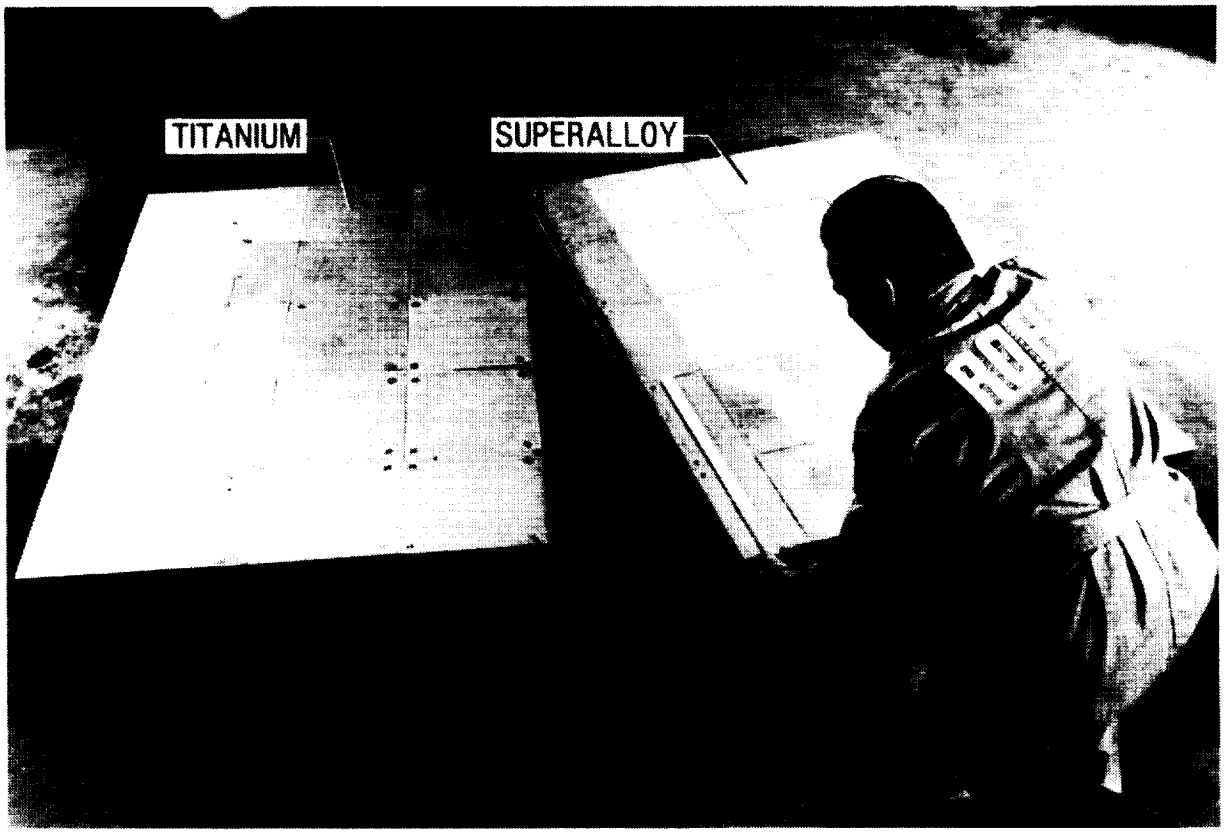

Figure 14

TITANIUM MULTIWALL 20-PANEL ARRAY IN LARC 8' HIGH TEMPERATURE TUNNEL

The titanium multiwall TPS 20-panel array mounted in the panel holder and installed in the 8' High Temperature Tunnel is shown in figure 15. The view is looking downstream in the tunnel. Fences attached to each side of the panel holder provide relatively uniform two-dimensional flow on the surface of the panel holder. The array of panels was installed so that the gaps between panels were parallel to the flow direction. This installation configuration is considered a "worst case" orientation of the panels with respect to the flow.

The insert in figure 15 shows a schematic view of the major components of the 8' High Temperature Tunnel, which is a "blow-down" tunnel. The model is held in a pod beneath the test section and covered by radiant heaters which not only preheat the model but also protect the model from tunnel start-up and shut-down loads. After the model is preheated and the tunnel is started, the radiant heaters are turned off and retracted by hydraulic actuators. The model is then rapidly inserted into the 8-foot-diameter test stream by a hydraulically-operated 15-ton elevator which raises the model to the test position in approximately 1 second. For shutdown, the procedure is reversed. The total aerothermal test duration is up to two minutes depending on test conditions.

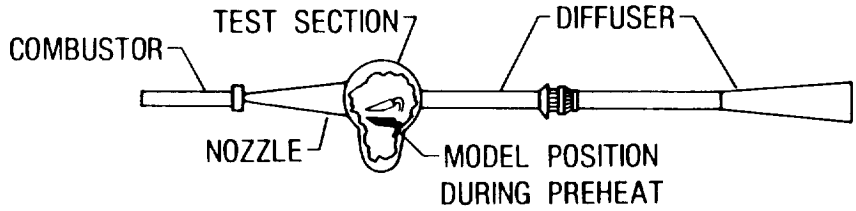

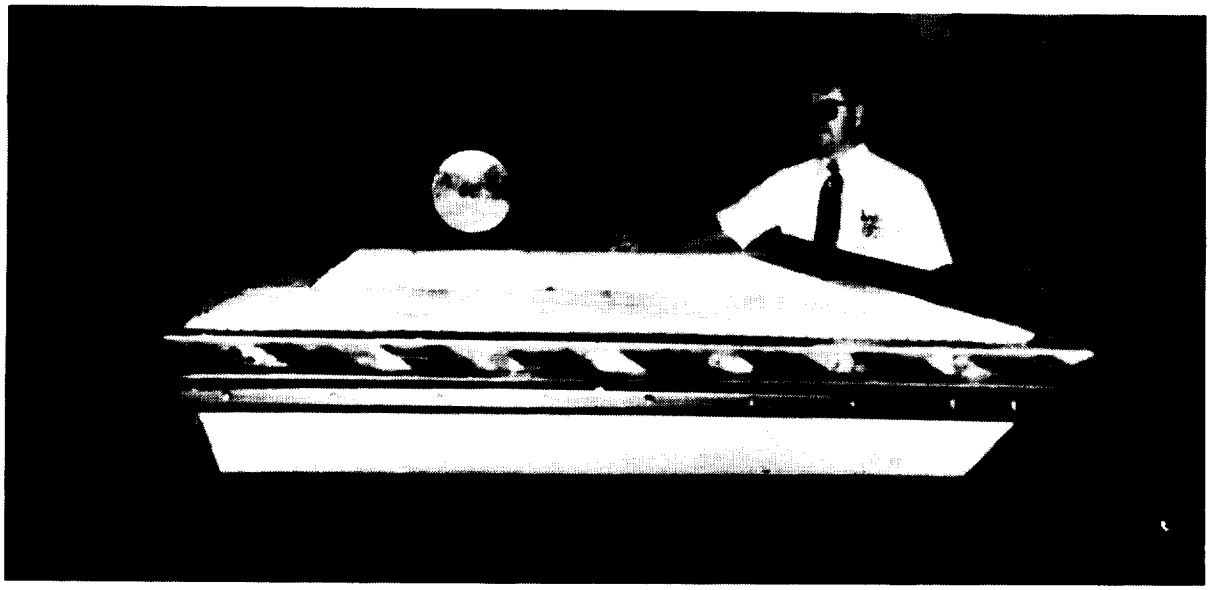

Figure 15

EFFECT OF AEROTHERMAL EXPOSURE ON GAP TEMPERATURE

One of the objectives of the aerothermal tests in the 8' High Temperature Tunnel was to determine if temperatures in the gaps between panels would be increased by exposure to the flow. Such an increase would indicate that the panel edge overlay covering the gap is not adequate by itself to prevent gap heating when the flow is parallel to the gap. Tests of an array of first-generation titanium multiwall panels indicated that flow did not occur in the gaps when the panels were oriented 30 degrees to the flow (ref. 8).

Surface temperatures and temperatures at the bottom of the gap are shown in figure 16 for both the titanium multiwall array and the superalloy honeycomb array. The dashed curves represent temperatures measured during a 200 second portion of an aerothermal test when the array was inserted into the tunnel stream. The solid curves represent temperatures recorded at the same locations and time intervals during a static radiant heating test.

For the time interval shown, the surface and gap temperatures of the titanium multiwall model were at equilibrium. When the model was inserted into the flow, negligible temperature change occurred at the bottom of the gap, thus indicating no additional gap heating occurred.

Although the surface of the superalloy honeycomb panel reached equilibrium, the temperature at the bottom of the gap was still approaching equilibrium when the radiant heaters were turned off and the model was inserted into the flow. Immediately after the superalloy model was inserted into the flow, the temperature at the bottom of the gap increased quickly. This high, quick temperature rise indicates that hot gases flowed into the gaps between the panels. Thus, when the edges of the superalloy panels are parallel to the flow, the overlapping edges did not provide an adequate seal. Superalloy honeycomb panels may be more susceptible to gap heating because the gap is much larger than the gap between titanium multiwall panels. Consequently, when thermal expansion closes the top of the gap, the bottom of the gap remains partly open because it is much cooler.

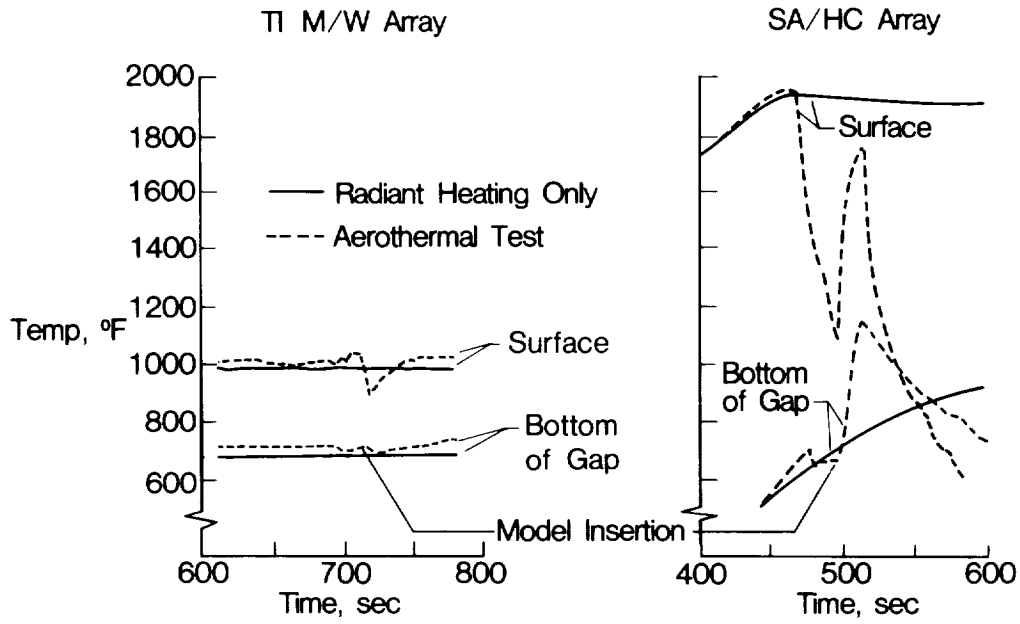

Figure 16

TEMPERATURE HISTORIES AT 4 GAP LOCATIONS

Even though the previous figure indicates that aerothermal heating in the gap between panels occurred at one location, the cause of such heating is not clear. The temperature histories at four gap locations for four different tests are shown in figure 17. In each of the four tests, the temperatures measured at the bottom of the gap at three different locations in the array (solid lines) increased rapidly when the model was inserted into the test stream. These temperatures were measured by thermocouples attached to the external surface of the side closure. However, the temperatures measured at a fourth location where the thermocouple was attached to the internal surface of the side closure (dashed lines) did not increase when the model was inserted into the stream. These results are consistent for all 4 tests and suggest that the presence of the thermocouple and thermocouple wire in the gaps between panels may have caused the heating in the gaps at those locations. Consequently, a definitive conclusion about the severity of aerothermal heating in gaps that are parallel to the flow is not possible at this time.

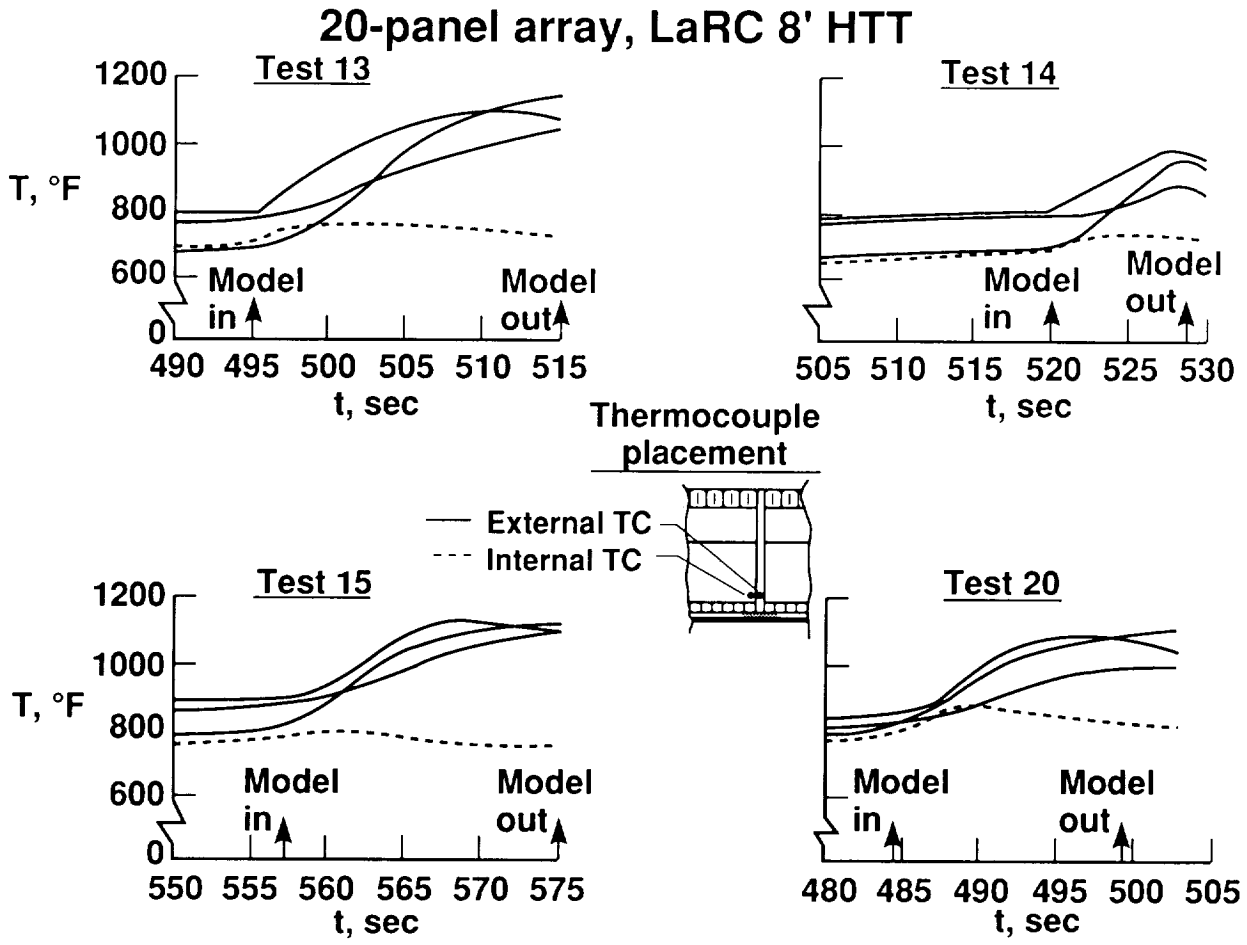

Figure 17

INTENTIONAL SURFACE DAMAGE TO SA/HC 20-PANEL ARRAY

The original test plan for the 20-panel arrays included aerothermal tests with the lightning-damaged panels included in the arrays. The lightning-damaged titanium multiwall panel was unchanged by the aerothermal test. Furthermore, a negligible increase in temperature (less than 10° F) occurred on the backside of the panel at the area of damage. Thus, lightning damage of the titanium multiwall concept does not appear to be a design concern.

The lightning-damaged superalloy honeycomb panel could not be installed into the array in a timely manner; therefore, panels already in the array were intentionally damaged to simulate the lightning damage. The types of damage inflicted on the panels are shown in figure 18. An opening was created in the outer surface of several panels by grinding, punching or burning with a torch. Additionally, one attachment plug was intentionally left out. The honeycomb core was left near the surface only at the torch burn-through. The two rows of panels in the foreground of figure 18, which were coated with a ceramic non-catalytic coating (ref. 9), were the panels that received the damage to the outer face sheet. (The dark panels in the background were coated with a high-temperature, high-emittance paint.) The array was then again exposed to aerothermal heating in the 8' High Temperature Tunnel.

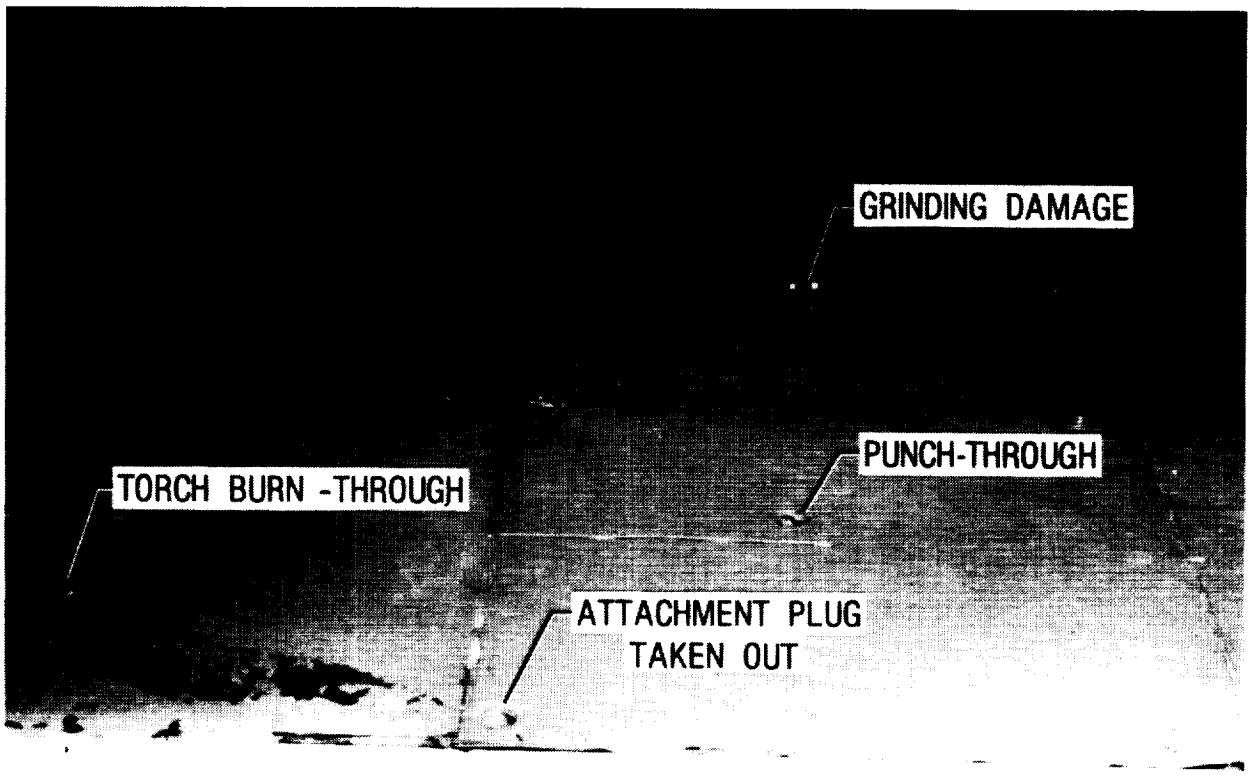

Figure 18

SA/HC 20-PANEL ARRAY IN 8' HIGH TEMPERATURE TUNNEL

The superalloy honeycomb 20-panel array with the intentionally damaged panels is shown in figure 19. The figure was made from a frame of movie film taken during the last aerothermal test of the array (run 20). The only light used to expose the film was that radiating from the model, which was at a temperature of about 1850° F. The thermal deflections of the heated model resulted in panel "pillowing", which caused slightly higher temperatures to occur on the upstream side than on the downstream side of the individual panels (ref. 10). The greater brightness (and higher temperature) of the right-hand side of the array (looking downstream) was caused by the lower emittance of the panels with the non-catalytic coating.

Several hot spots can be seen where the face sheet buckled and delaminated from the honeycomb core. The damage occurred early in the test program when fiberglass curtains, used to protect surrounding structure from radiation from the quartz heaters, melted and fell on the panels. The buckles and delaminations did not propagate during the balance of the test program. A hot spot was caused by the torch burn-through discussed in figure 18. This hot spot may have occurred because the exposed honeycomb core was near the flow stream. The other two damaged locations and the open attachment hole did not appear to cause any significant overheating. Bent gap covers also appeared as hot spots since they protrude into the airflow. The gap covers in the rear of the model were in contact with the rigid Glassrock material that surrounded the array and were deformed when the panels bowed thermally. The single gap cover hot spot that occurred at the intersection of four panels was probably caused by thermal bowing interference between panels with different attachments. This location was the only intersection where a bayonet-clip-attached panel overhung a panel with through-panel attachments.

Post-test inspection of the array was not possible because, at the end of this test, part of the panel holder broke and caused the tunnel to "unstart". The strong shock wave (10 psi pressure rise in about 0.2 seconds) passing through the test section completely destroyed the array of panels, which were designed for 2 psi.

RUN 20

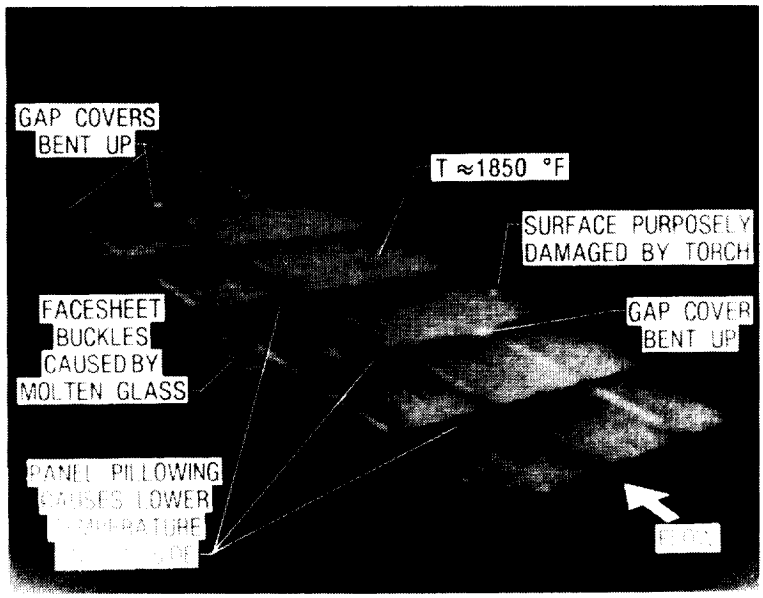

Figure 19

NON-CATALYTIC COATING ARC-TUNNEL TEST RESULTS

For the same entry conditions, a metallic surface of an entry vehicle will be subjected to a higher heating rate than a nonmetallic surface. This difference occurs because oxides of high-temperature structural metals are generally catalytic to the recombination of dissociated air molecules, and the energy of dissociation released during recombination adds to the heat load (ref. 11). A non-catalytic coating will reduce the heat load to the surface and greatly increase the thermal efficiency of metallic TPS.

A commercially available, water-base, silica-alumina ceramic coating was evaluated by exposing coated and uncoated Inconel 617 specimens in the LaRC 1 MW Aerothermal Arc Tunnel using air as a test medium. Prior to the arc tunnel tests, the emittances of the specimens were measured, and coated specimens were subjected to 80 thermal shock cycles in a 2000° F furnace to evaluate the adhesion of the coating to the metal (ref. 9). The measured emittance of the coated and uncoated (but oxidized) specimens were 0.65 and 0.8, respectively. The coating remained attached during the thermal shock cycles, and the emittance did not change.

The results of the arc tunnel tests are shown in figure 20. Arc tunnel test conditions were established that resulted in a temperature of 1753° F on the uncoated specimen. The coated specimen was tested at the same condition, but reached only 1353° F. Modification of the coating composition to increase surface emittance without harming the non-catalytic and adherence characteristics would further reduce the temperature. Radiation equilibrium heating rates were calculated using the maximum measured surface temperatures and the measured emittances. The heating rate on the coated specimen was only 37 percent of the heating rate on the uncoated specimen.

This coating was applied to several superalloy honeycomb TPS test panels exposed to wind tunnel, thermal/vacuum, lightning strike, vibration, and acoustic tests. Results from these tests further indicate that the non-catalytic coating adheres well. Thus, an adhering, non-catalytic coating is feasible and should be used for metallic TPS; however, emittance greater than 0.65 is desirable.

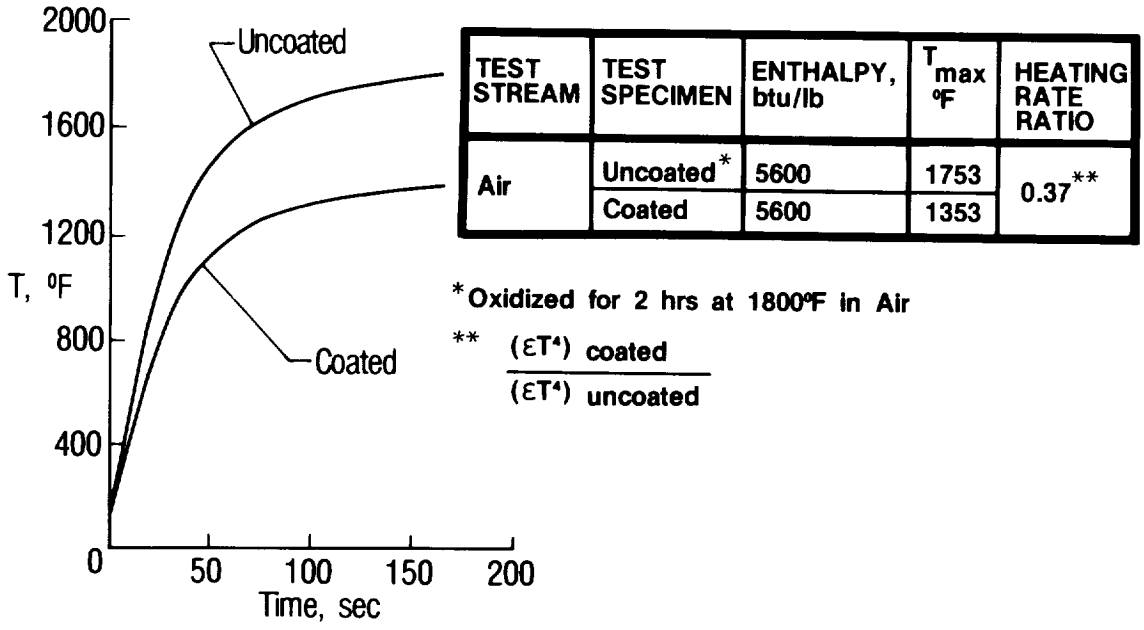

TEST STREAM	TEST SPECIMEN	ENTHALPY, btu/lb	T_{max} °F	HEATING RATE RATIO
Air	Uncoated*	5600	1753	0.37**
	Coated	5600	1353	

*Oxidized for 2 hrs at 1800°F in Air

** $\frac{(\varepsilon T^4)\ \text{coated}}{(\varepsilon T^4)\ \text{uncoated}}$

Figure 20

EFFECT OF CURVATURE ON THERMAL STRESS OF UNCONSTRAINED PANEL

One of the main differences between the design of flat and curved TPS is the effect of curvature on thermal stress. The thermal stresses in an unconstrained TPS structure are zero if the temperature distributions through the structure are linear when they are measured in a rectangular Cartesian coordinate system (ref. 12). The flat panel shown in figure 21 has a linear temperature distribution through the depth, and since this distribution results in a linear (constant in this instance) temperature distribution in the plane *z=constant*, no thermal stress occurs. However, the same linear temperature distribution through the depth of the curved panel shown in the figure results in a nonlinear temperature distribution in the plane *z=constant*. Consequently, thermal stresses occur in the curved panel even if the temperature distribution through the depth is assumed to be linear.

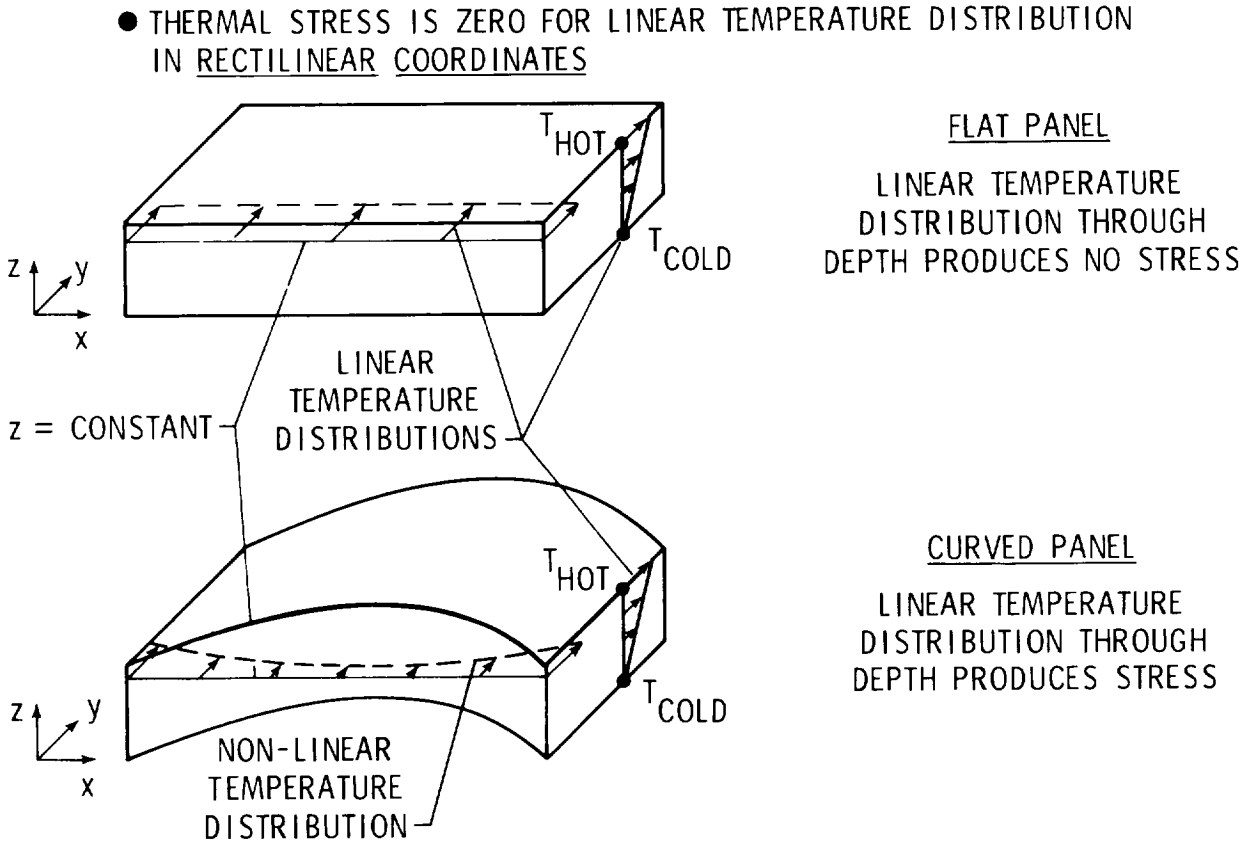

Figure 21

SPAR FINITE ELEMENT MODEL OF SA/HC TPS

The SPAR finite element structural analysis computer program (ref. 13) was used to study thermal stress in a curved TPS panel. The thickness of the panel was 2.35 inches, and the radius of curvature was 12 inches. The nominal size of the panel analyzed was 12 inches long and 9.42 inches wide (measured in the direction of curvature). By using planes of symmetry, only 1/4 of a panel needed to be modeled. As shown in figure 22, the outer superalloy honeycomb sandwich (0.280 inches thick) and inner titanium honeycomb sandwich (0.170 inches thick) were modeled using membrane elements for the face sheets and solid elements for the cores. The Inconel 617 side closures were modeled using rod elements and shear elements. The model had 745 elements and 520 nodes. The model was unconstrained from deformations except for rigid body displacements and rotations.

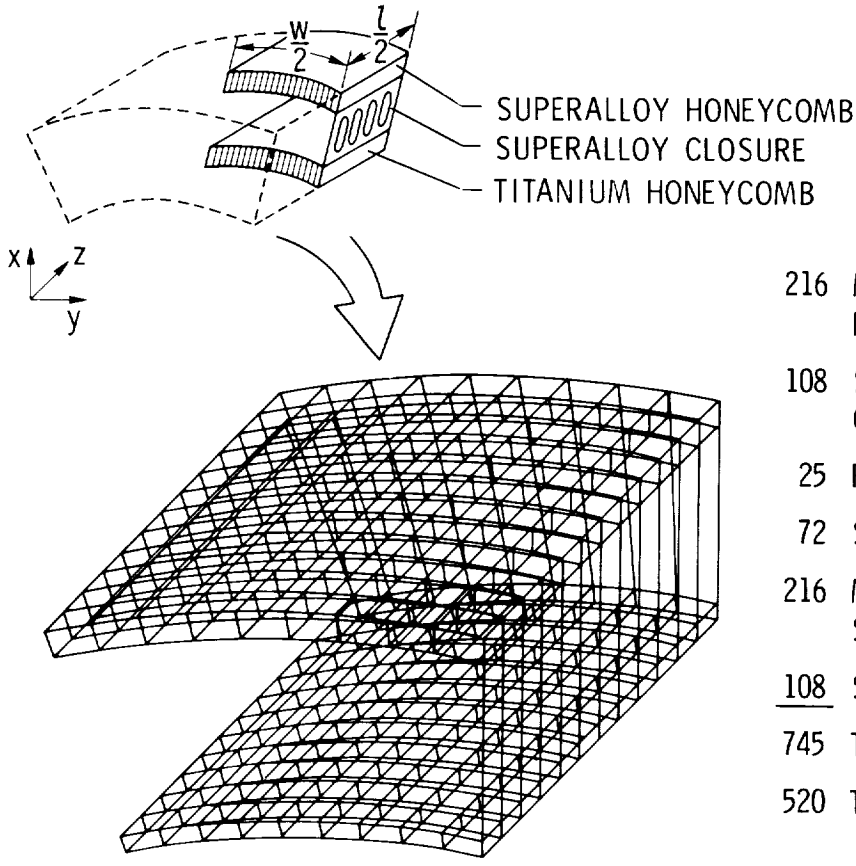

ELEMENTS

216	MEMBRANES — INCO FACE SHEETS	
108	SOLIDS — INCO H/C CORE	
25	RODS	INCO SIDE CLOSURES
72	SHEAR	
216	MEMBRANES — Ti FACE SHEETS	
108	SOLIDS — Ti H/C CORE	
745	TOTAL ELEMENTS	
520	TOTAL NODES	

Figure 22

TEMPERATURES FOR FINITE ELEMENT ANALYSIS

The surface temperature history associated with Space Shuttle trajectory 14414.1C at body point 1300 (ref. 3) was used as a typical design condition to calculate temperatures for the finite element thermal stress analysis. The panel cross section in figure 23 shows the Inconel 617 honeycomb, the titanium honeycomb, two types of fibrous insulation contained within the panel, and the aluminum plate which is sized to represent the thermal mass of Shuttle structure at body point 1300. The symbols on the sketch to the right of the cross section identify 5 of the 18 locations used in a one-dimensional thermal analysis modified to account for the side closures. Two of the symbols represent temperatures of the Inconel face sheets; two of the symbols represent temperatures of the titanium face sheets; and one symbol represents the temperature of the aluminum plate. The analysis of reference 3 used the MITAS finite difference computer program.

The maximum temperature difference through the thickness of the panel occurs at about 500 seconds when the surface temperature reaches 1900° F. The inner superalloy face sheet is at 1875° F, and the titanium face sheets are both at about 200° F. These face sheet temperatures were applied at the appropriate nodes of the finite element model. The temperature distribution was assumed to be uniform for each face sheet.

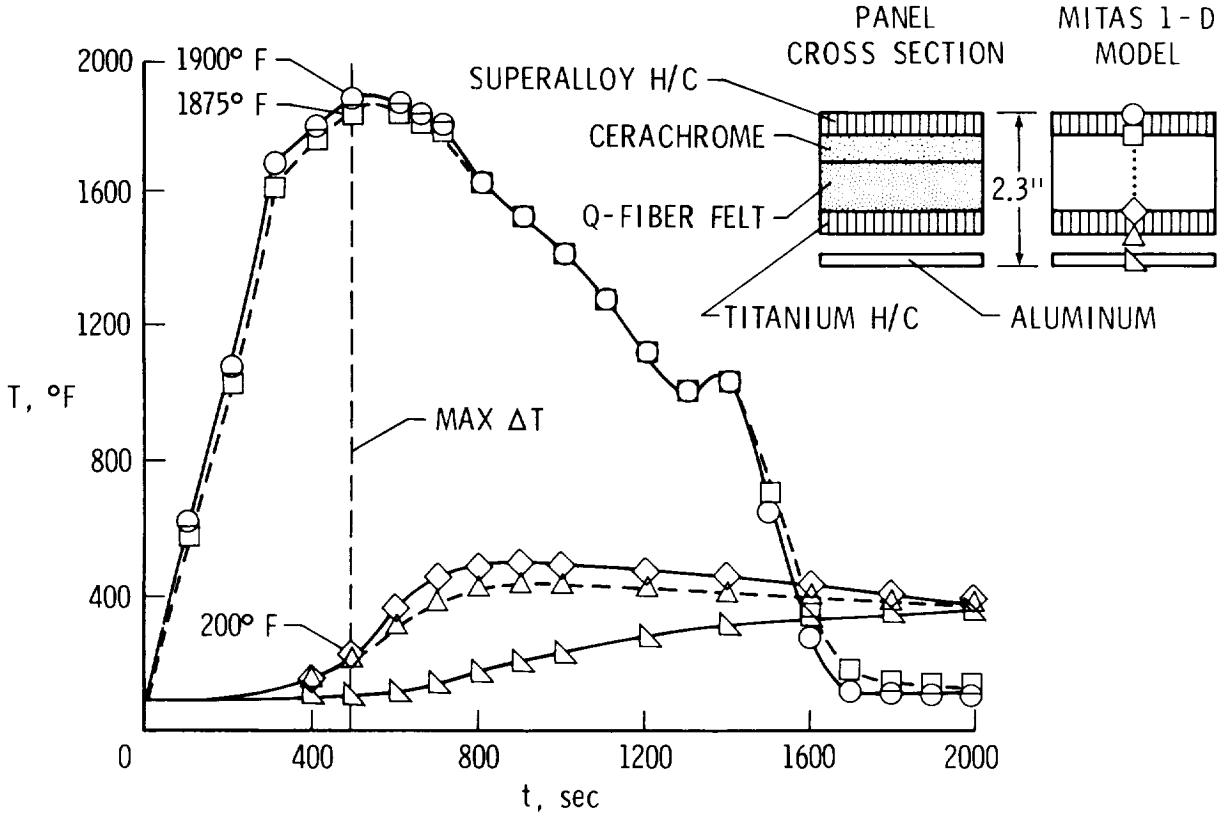

Figure 23

COMPRESSIVE STRESS IN INCONEL 617 HONEYCOMB INNER FACE SHEET

Thermal stresses for the curved panel were calculated using a linear elastic analysis (See fig. 22) with the temperatures described in figure 23 as the applied load. The highest compressive inplane stresses, indicated by the heavy line in the sketch shown in figure 24, were along the edge of the inner face sheet adjacent to the side closure. These stresses reached a maximum at the center of the side closure. The stresses are normalized by the yield stress for Inconel 617 at 1875° F determined for 0.005-inch-thick material which has experienced the braze cycle (ref. 3). The maximum stress calculated for a 12-inch-long panel is 2.3 times greater than the yield stress. Reducing the length of the panel by half while maintaining the 9.42-inch width lowered the maximum stress to a value slightly less than the yield stress. (Reducing the width of the panel by half while maintaining the 12-inch length only lowered the maximum stress to 1.7 times yield.)

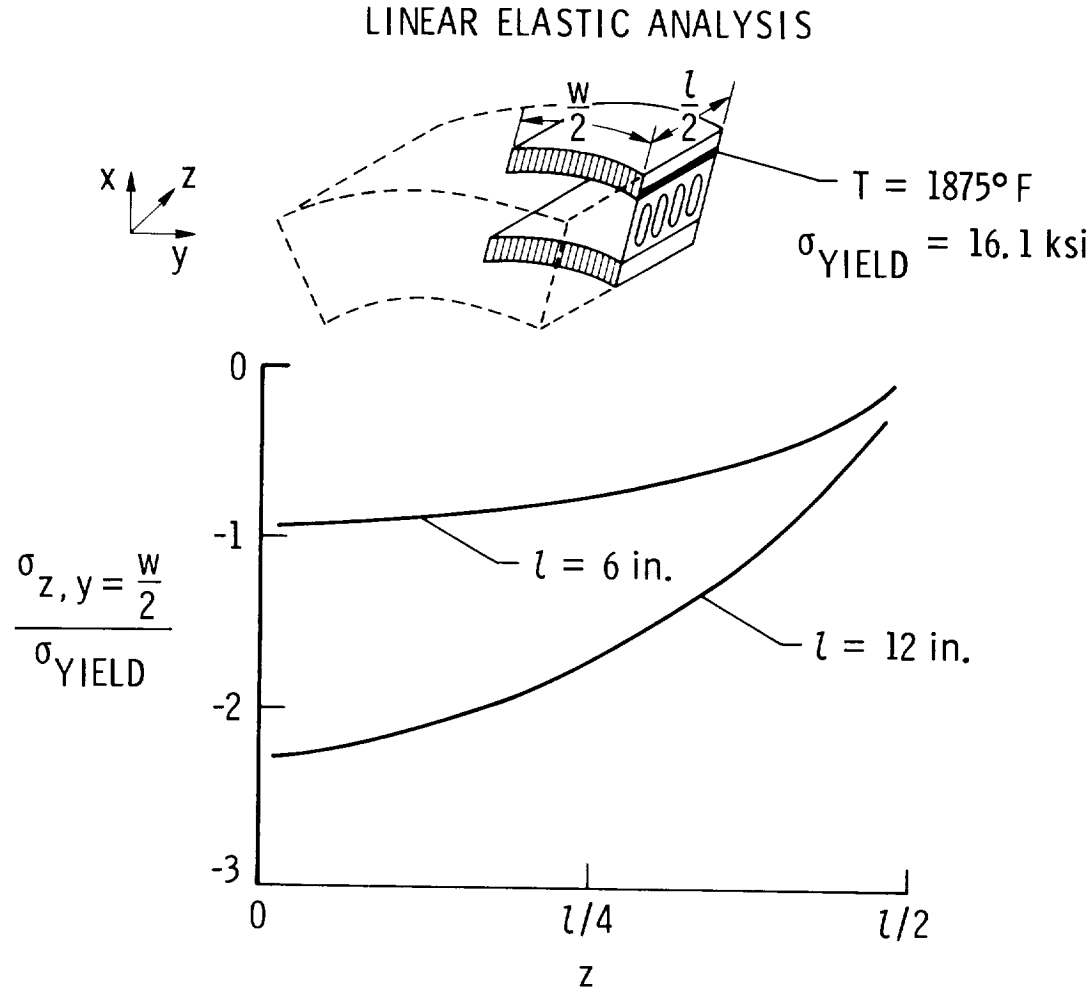

Figure 24

SHEAR STRESS IN INCONEL 617 HONEYCOMB INNER FACESHEET

Inplane shear stresses computed for the same location that was described in figure 24 are shown in figure 25. Shear stresses for the 12-inch-long, 9.42-inch-wide panel have maximum values of about 1.5 times yield stress, while stresses for a 6-inch-long panel were reduced to a value slightly less than yield. Therefore, both compressive stresses (fig. 24) and shear stresses were found to be more sensitive to a change in length than to a change in width. Thus, one way to control thermal stresses in curved TPS panels is to adjust the length of the panels.

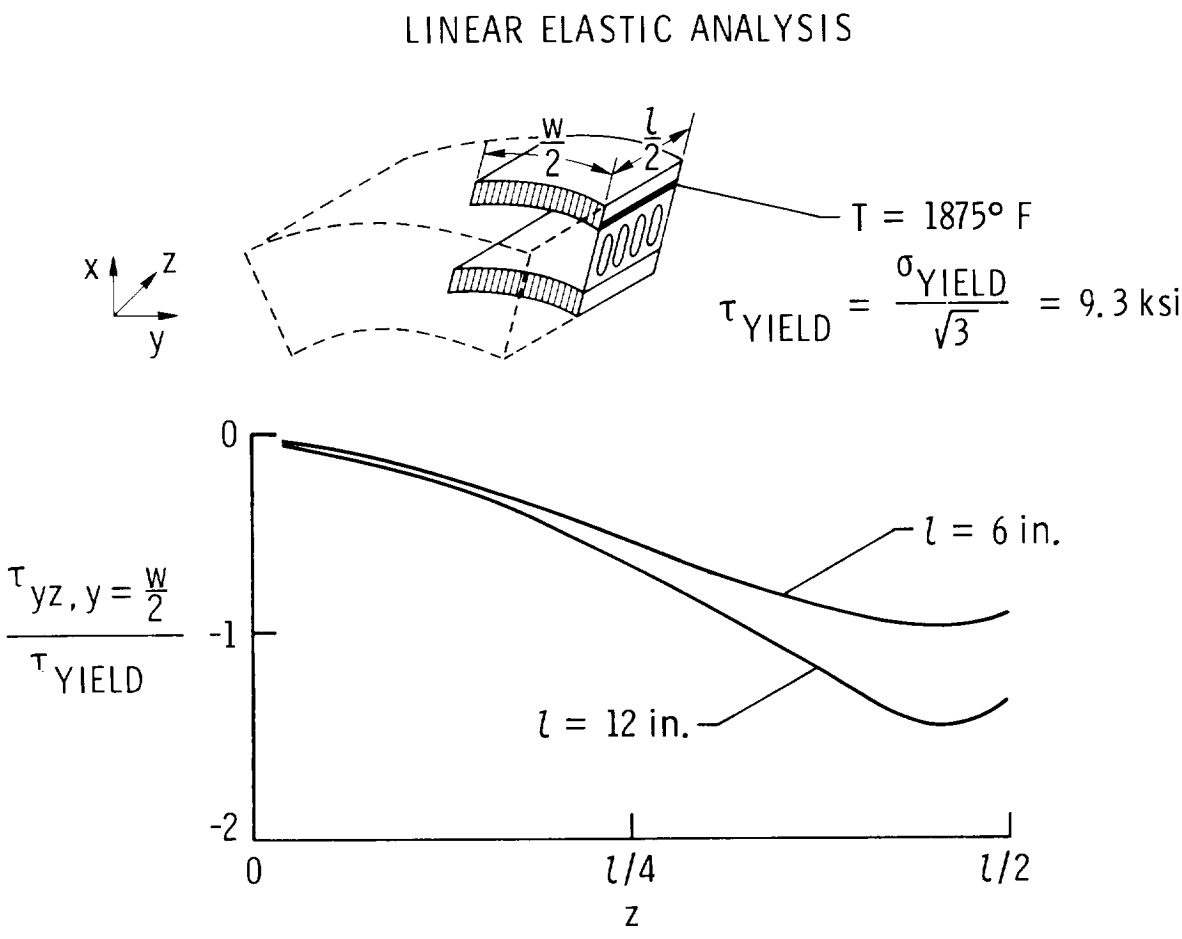

Figure 25

EFFECT OF NONLINEAR MATERIAL PROPERTIES ON THERMAL STRAIN

Even though the linear elastic analysis of a 12-inch-long panel indicated a maximum stress 2.3 times greater than yield stress, the strain associated with that stress (0.00282 in./in.) is less than the yield strain. Since thermal stress is induced by an applied strain (as opposed to an applied force), the strain calculated from a nonlinear analysis would be expected to also be about 0.00282 in./in.). As illustrated in figure 26, the stress and strain would be slightly less than yield conditions. Even if a full strain range of 0.00282 in./in. is assumed, the fatigue life calculated from the equation on the right in the figure (method of universal slopes with a 10 percent rule, ref. 14) is 1800 cycles. This life is adequate for space transportation vehicles that experience only one thermal cycle per mission.

Thus, two methods exist to control thermal stress in curved TPS panels. First, the size can be reduced as discussed previously, and second, plastic deformation can be allowed to occur at least on the first cycle, after which the remaining cycle life may be adequate.

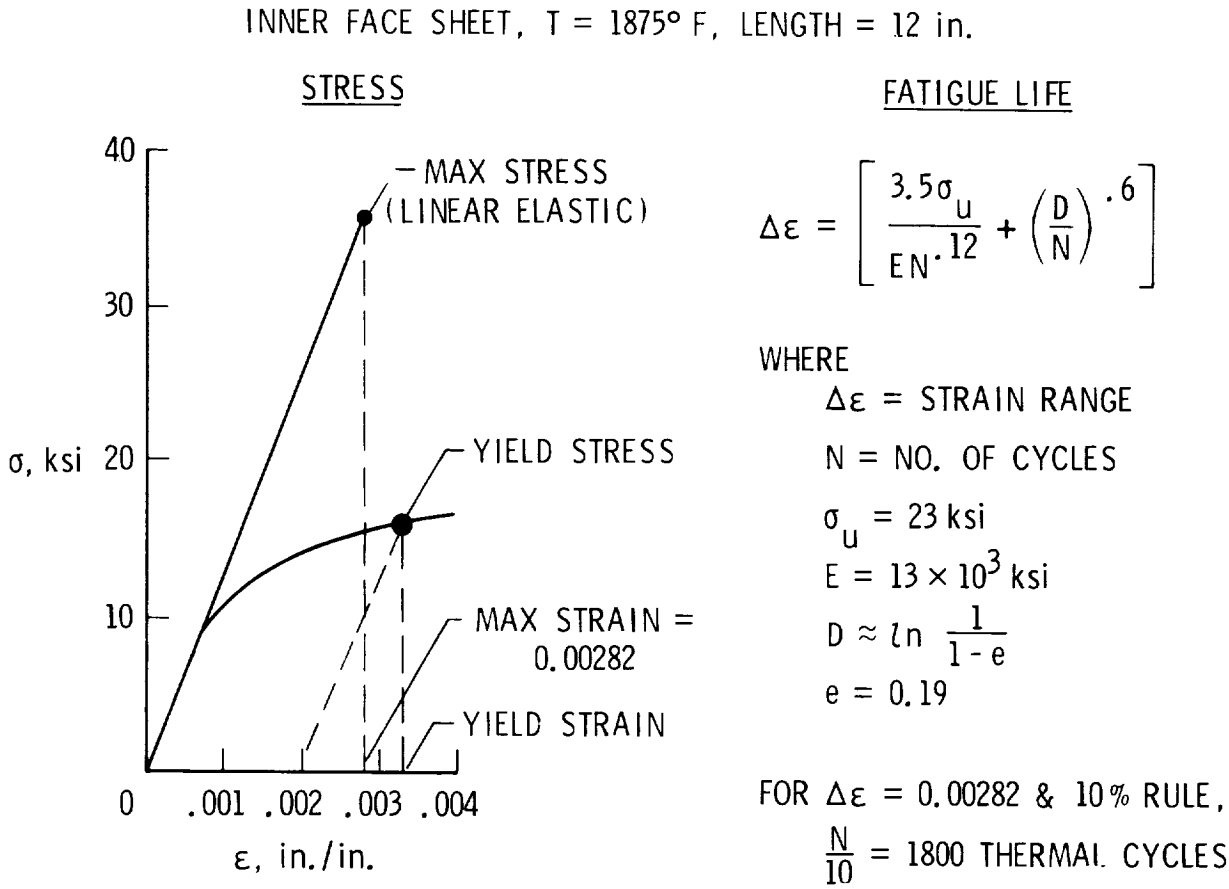

Figure 26

CURVED SUPERALLOY HONEYCOMB TPS PANELS

Even though much of the surface of Shuttle-type vehicles is flat or nearly flat, some locations, such as the chine areas, are necessarily curved. The fabrication of curved TPS panels often presents complexities not encountered in fabricating flat panels. A curved titanium multiwall panel was fabricated to demonstrate that the multiwall concept will lend itself to curved panels. A single curved superalloy honeycomb panel (fig. 27) has been fabricated, instrumented with thermocouples and strain gages, and exposed to radiant heat to determine thermal stresses. Reliable measured thermal strains have not been obtained for this panel because the very thin material (0.005-in.-thick face sheets and 0.003-in.-thick beaded side closures) deforms in local bending under very low load. Consequently, evaluation of the structural behavior of the curved panel in these tests may be limited to deflection measurements and post-test inspection.

The design of curved panels must include not only factors contributing to thermal stress but must also consider the effects of large surface pressure gradients that are normally less important in the design of flat TPS. An array of curved superalloy panels has been fabricated for aerothermal tests to evaluate their performance in a high-surface-pressure-gradient environment. The curved 20-panel array shown in figure 27 was installed into the cavity of the Curved Surface Test Apparatus (CSTA), so that the surface of the array was flush with the surface of the CSTA. The array was instrumented with thermocouples and pressure sensors and tested in the LaRC 8' High Temperature Tunnel to determine if heating would occur in the gaps between panels. Metal tabs, one of which is identified on the single panel in the figure, were located at the corner intersections of the panels to block flow in the gaps. All of the panels were attached with through-panel fasteners.

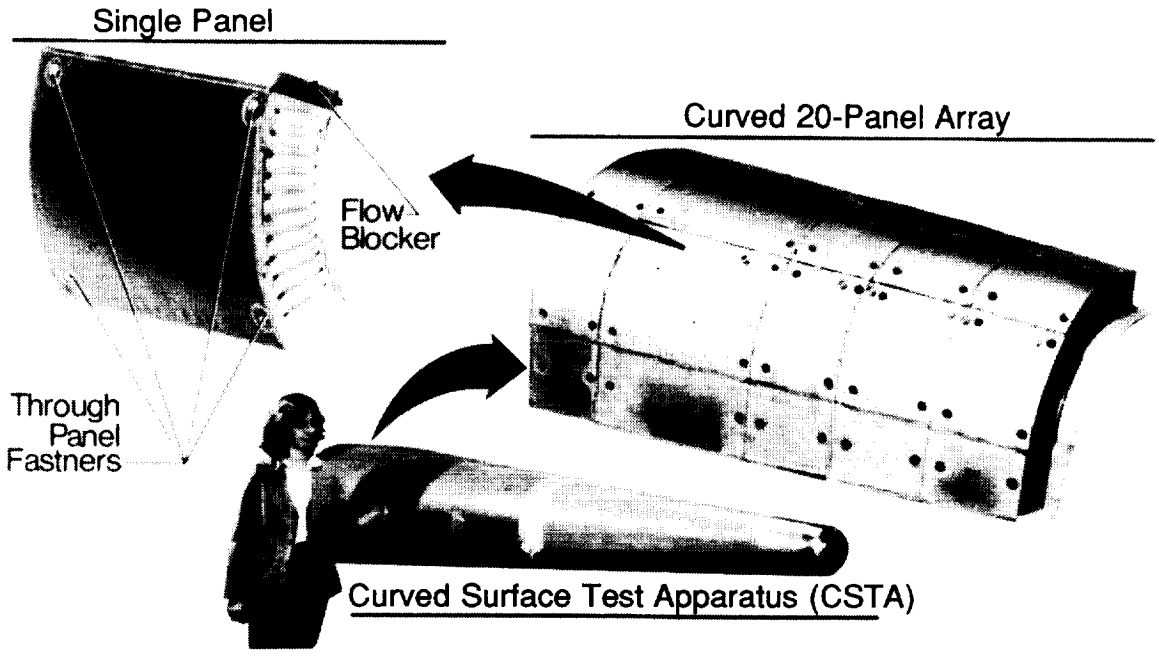

Figure 27

AEROTHERMAL TEST OF CURVED SUPERALLOY HONEYCOMB PREPACKAGED TPS

After the windward panels of the curved array were preheated with quartz lamps to a surface temperature of 2000° F, the array was exposed for 34 seconds to the most severe conditions that are within the normal operating range of the 8' High Temperature Tunnel. The tunnel dynamic pressure was approximately 1400 psf, and the pressure gradient along the curved surface of the array was approximately 2 psi per foot. The view on the left of figure 28 shows the array when it first reached the center of the hypersonic stream. Although the surface of the panels had cooled during the time the quartz lamps were turned off and the model was being inserted, the fastener plugs, which have high thermal mass compared to the panel face sheets, are still glowing. The view on the right of the figure shows the array after exposure to the flow for 34 seconds. The maximum surface temperature on the windward panels was approximately 1800° F. Post-test examination of the array revealed that panels near the aft seal of the cavity into which the panels were installed were damaged and that the seal had failed. Failure of the cavity seal allowed the hot gas at the surface of the panels to flow directly through the gaps between panels and through the seal to the base of the model. Consequently, no definitive conclusions can be made from these test results regarding gap heating.

The damaged panels in the array have been repaired, and the aft seal of the cavity, which was a sliding seal, has been replaced with a more positive, bellows-type seal. The array is currently available to be tested in the 8' High Temperature Tunnel.

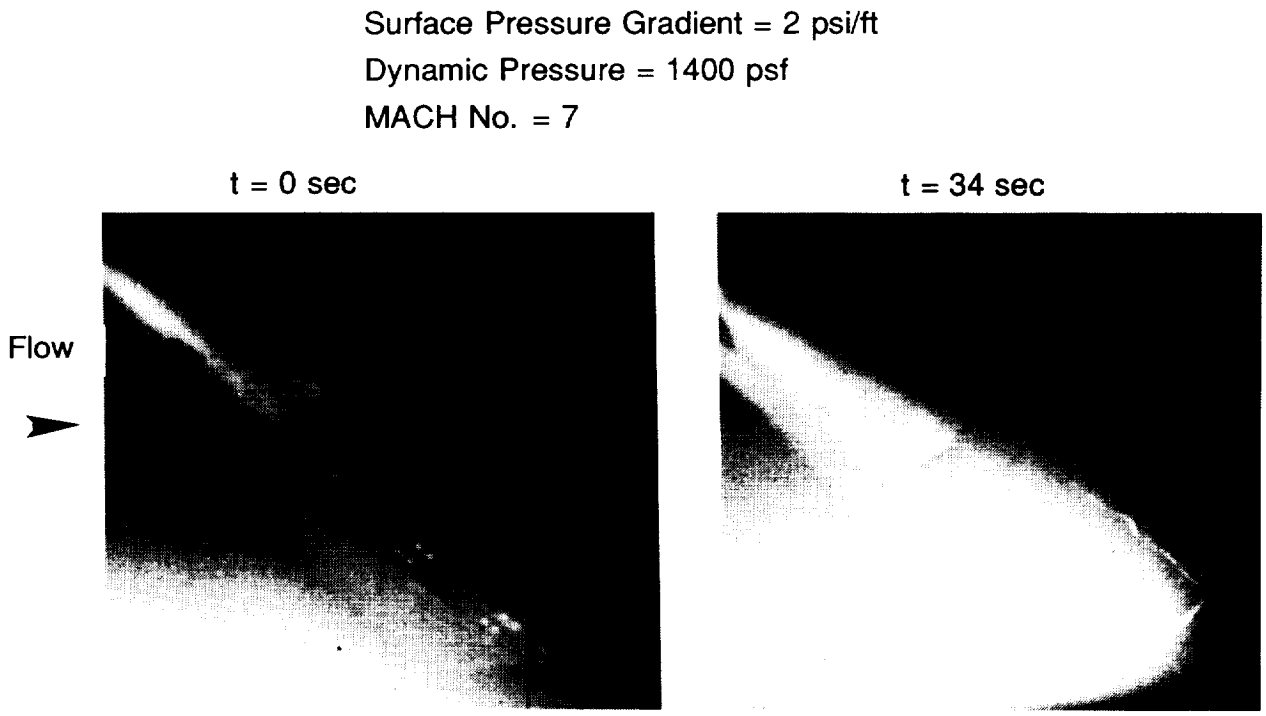

Figure 28

ACC MULTIPOST TPS TEST ARTICLE

The same 1 ft. by 2 ft. ACC test model that was subjected to the thermal vacuum tests (fig. 7) was also subjected to aerothermal tests. The model, shown in figure 29, was instrumented with thermocouples through the thickness directly beneath the center portion where four panel corners intersect.

Figure 29

ACC MULTIPOST TPS IN ARC-TUNNEL

The ACC test model is shown in figure 30 installed in the LaRC 20-MW Aerothermal Arc Tunnel. The model was mounted in a water-cooled holder at 15° angle of attack to the air stream with a 6-inch transition section between the nozzle and the model. Conditions were selected which gave a 2300° F surface temperature on the front of the model. Figure 6 (e) shows the model in the test stream. Only the light being radiated from the model was used to expose the film.

Figure 30

EFFECT OF AEROTHERMAL EXPOSURE ON GAP TEMPERATURE ACC MULTIPOST

A comparison of temperatures obtained during the arc-tunnel tests with those obtained during a thermal/vacuum test is shown in figure 31. The temperatures shown were measured at the center of the model where pieces of 4 separate panels intersect. Thermocouples placed at locations 1, 2, and 3 of the lower right-hand sketch measured the temperature at the ACC skin, at 1/3 of the depth of the model, and at the bottom of the model, respectively. The tunnel condition resulted in a surface temperature (location 1) nearly 100° F less than that obtained during the thermal/vacuum test. However, the temperature measured at location 2 during the arc-tunnel test was not less than that obtained during the thermal vacuum test, indicating that slight heating due to flow occurred in the gap region where one panel overlaps another. The lower temperature measured near the aluminum plate (location 3) during the tunnel test was encountered at other locations and probably reflects a larger heat-sink effect caused by a water-cooled holder which was not used in the thermal/vacuum tests. These results suggest modifications to the concept to reduce the local heating at the ACC panel intersections that include not only staggering the insulation packages so that they do not coincide with the panel intersections but also eliminating the vertical flanges that conduct heat into the insulation.

The ACC panel was not damaged by either the thermal/vacuum or arc-tunnel tests. The only change in appearance occurred during the arc-tunnel tests when erosion of copper electrodes caused an orange-colored copper deposit on part of the panel surface (fig. 30).

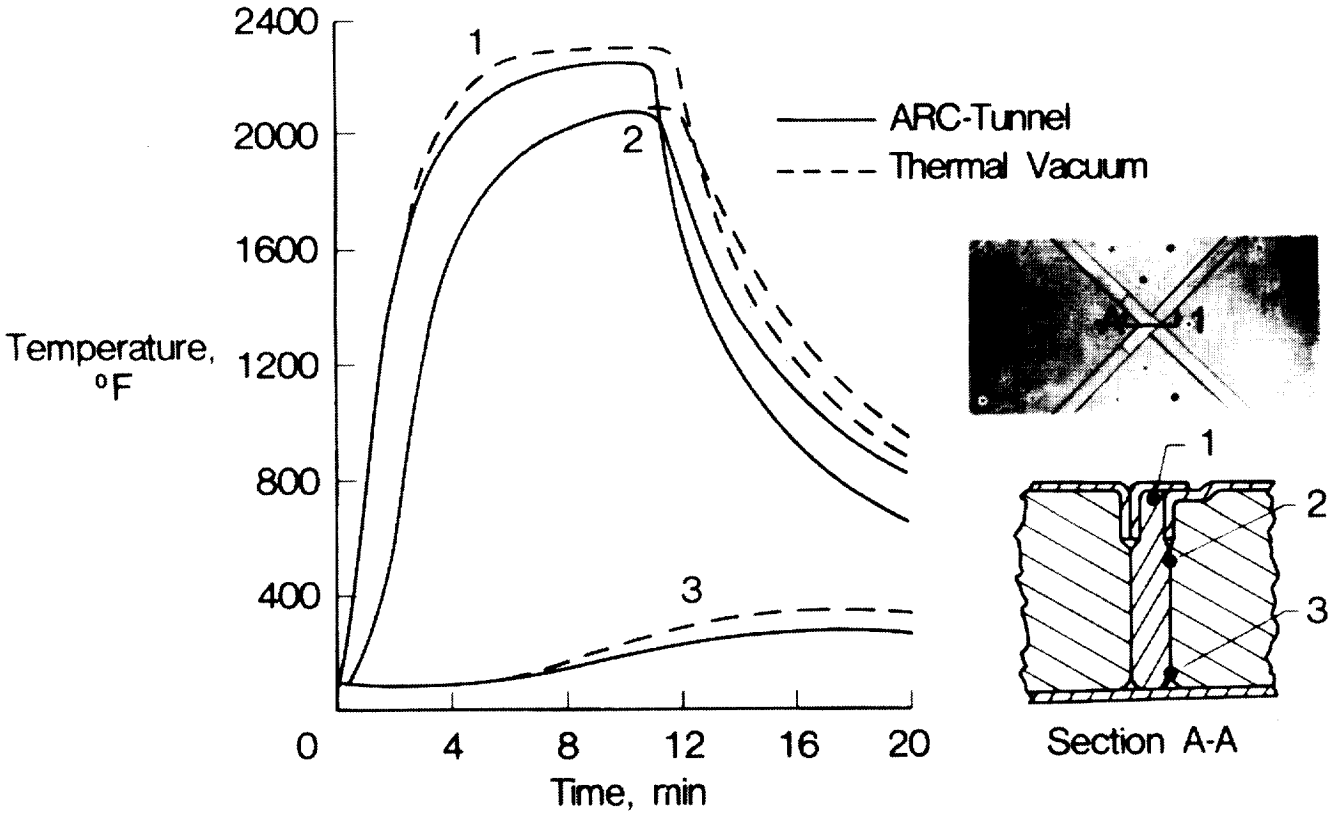

Figure 31

SUMMARY

The results from a variety of verification tests, including thermal, aerothermal, vibration, acoustic, lightning strike, and environmental exposure, indicate that the three TPS concepts (titanium multiwall, superalloy honeycomb prepackaged, and ACC multipost) are viable over a temperature range from 700° F to a temperature greater than 2300° F. However, the application of these concepts to specific vehicles will require additional verification tests dedicated to specific mission requirements.

- **Results from verification tests indicate TPS concepts are weight competitive and are adequate for generic entry environments**
  - **Thermal**
  - **Aerothermal**
  - **Vibration**
  - **Acoustic**
  - **Lightning strike**
  - **Environmental exposure**
- **Application to specific vehicles will require additional verification tests dedicated to specific mission requirements**

Figure 32

REFERENCES

1. Bohon, Herman L.; Shideler, John L.; and Rummler, Donald R.: Radiative Metallic Thermal Protection Systems: A Status Report. Journal of Spacecraft and Rockets, Vol. 14, No. 10, pp. 626-631, October 1977.

2. Blair, W.; Meany, J.E.; and Rosenthal, H.A.: Re-Design and Fabrication of Titanium Multiwall Thermal Protection System (TPS) Test Panels. NASA CR-172247, 1984.

3. Blair, W.; Meany, J.E.; and Rosenthal, H.A.: Fabrication of Prepackaged Superalloy Honeycomb Thermal Protection System (TPS) Panels. NASA CR-3755, 1985.

4. While, D.M.: ACC Cover Panel Feasibility Study. In Development of Advanced Carbon-Carbon (ACC) Composites, Vol. II. NASA CR-165842-2, July 1982.

5. Matza, E.C.; and While, D.M.: Advanced Carbon-Carbon (ACC) Test Article Design and Fabrication. Vought Corp. Report 221RPTA018, May 1983.

6. Pittman, Claud M.; and Brinkley, Kay L.: One-Dimensional Numerical Analysis of the Transient Thermal Response of Multilayer Insulation Systems. NASA TMX 3370, April 1976.

7. Anon.: Lightning Test Waveforms and Techniques for Aerospace Vehicles and Hardware. Report of SAE Committee AE4L, June 20, 1978.

8. Avery, D.E.; Shideler, J.L.; and Stuckey, R.N.: Thermal and Aerothermal Performance of a Titanium Multiwall Thermal Protection System. NASA TP 1961, December 1981.

9. Pittman, C.M.; Brown, R.D.; and Shideler, J.L.: Evaluation of a Non-Catalytic Coating for Metallic TPS. NASA TM 85745, January 1984.

10. Olsen, G.C.; and Smith, R.E.: Analysis of Aerothermal Loads on Spherical Dome Protuberances. AIAA Paper 83-1557, June 1983.

11. Greaves, J.C.; and Linnett, J.W.: "Recombination of Atoms at Surfaces", Part 5: Oxygen Atoms at Oxide Surfaces. Transactions of the Faraday Society, Volume 55, 1959, p. 1346.

12. Boley, B.A.; and Weiner, J.H.: Theory of Thermal Stress. John Wiley and Sons, New York, 1960.

13. Anon.: SPAR Structural Analysis System Reference Manual, Volume 1. NASA CR-158970-1, December 1978.

14. Manson, S.S.: A Simple Procedure for Estimating High-Temperature Low-Cycle Fatigue. Experimental Mechanics, August 1968.